

Olefin Polymerization by Dinuclear Zirconium Catalysts Based on Rigid Teraryl Frameworks: Effects on Tacticity and Copolymerization Behavior

Jessica Sampson[†], Gyeongshin Choi[†], Muhammed Naseem Akhtar[‡], E.A. Jaseer[‡], Rajesh Theravalappil[‡], Hassan Ali Al-Muallem[†], Theodor Agapie[†]

[†]Division of Chemistry and Chemical Engineering, California Institute of Technology, Pasadena, CA 91125, United States.

[‡]Center for Refining and Petrochemicals, King Fahd University of Petroleum and Minerals, Dhahran, 31261, Saudi Arabia.

[†]Department of Chemistry, King Fahd University of Petroleum and Minerals, Dhahran, 31261, Saudi Arabia.

Supporting Information

Contents

<i>Experimental Details</i>	S3
Synthesis of tetrabenzylzirconium	S3
Synthesis of compounds 5 , 6 , and 15	S3
Synthesis of compound 7	S3
Synthesis of $\text{H}_2^{\text{tBuSiPr}_3}\text{-NMe}_2$	S4
Synthesis of $\text{Zr}_1^{\text{tBuSiPr}_3}\text{-NMe}_2$	S4
Synthesis of compound anth2	S4
Synthesis of compound anth3	S5
Synthesis of compound anth4	S5
Synthesis of compound anth8	S6
Synthesis of compound anth9	S6
Synthesis of compound anth10	S6
Synthesis of compound 17	S7
Synthesis of compound 18	S7
 <i>NMR Characterization</i>	 S8
Figure S1. ^1H NMR spectrum of $\text{H}_4^{\text{SiPr}_3}\text{-NMe}_2$ in CDCl_3	S8
Figure S2. $^{13}\text{C}\{^1\text{H}\}$ NMR spectrum of $\text{H}_4^{\text{SiPr}_3}\text{-NMe}_2$ in CDCl_3	S8
Figure S3. ^1H NMR spectrum of $\text{C}_5\text{Zr}_2^{\text{SiPr}_3}\text{-NMe}_2$ in C_6D_6	S8
Figure S4. $^{13}\text{C}\{^1\text{H}\}$ NMR spectrum of $\text{C}_5\text{Zr}_2^{\text{SiPr}_3}\text{-NMe}_2$ in C_6D_6	S9
Figure S5. ^1H NMR spectrum of $\text{C}_5\text{Zr}_2^{\text{SiPr}_3}\text{-NMe}_2$ in CD_2Cl_2	S9
Figure S6. gCOSY spectrum of $\text{C}_5\text{Zr}_2^{\text{SiPr}_3}\text{-NMe}_2$ in CD_2Cl_2	S10
Figure S7. ^1H NMR spectrum of $\text{C}_2\text{Zr}_2^{\text{SiPr}_3}\text{-NMe}_2$ in C_6D_6	S10
Figure S8. $^{13}\text{C}\{^1\text{H}\}$ NMR spectrum of $\text{C}_2\text{Zr}_2^{\text{SiPr}_3}\text{-NMe}_2$ in C_6D_6	S11
Figure S9. ^1H NMR of $\text{C}_2\text{Zr}_2^{\text{SiPr}_3}\text{-NMe}_2$ in CD_2Cl_2	S11
Figure S10. gCOSY of $\text{C}_2\text{Zr}_2^{\text{SiPr}_3}\text{-NMe}_2$ in CD_2Cl_2	S12
Figure S11. ^1H NMR spectrum of $\text{H}_2^{\text{ArSiPr}_3}\text{-NMe}_2$ in CDCl_3	S12
Figure S12. $^{13}\text{C}\{^1\text{H}\}$ NMR spectrum of $\text{H}_2^{\text{ArSiPr}_3}\text{-NMe}_2$ in CDCl_3	S13

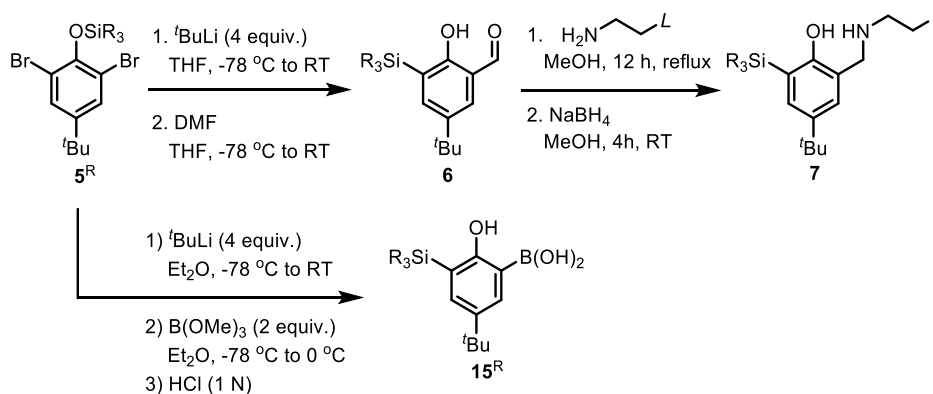
Figure S13. ^1H NMR spectrum of $\text{Zr}_1^{\text{ArSiPr}_3}\text{-NMe}_2$ in C_6D_6	S13
Figure S14. $^{13}\text{C}\{^1\text{H}\}$ NMR spectrum of $\text{Zr}_1^{\text{ArSiPr}_3}\text{-NMe}_2$ in C_6D_6	S13
Figure S15. ^1H NMR spectrum of $\text{anthH}_4^{\text{SiPr}_3}\text{-NMe}_2$ in CDCl_3	S14
Figure S16. $^{13}\text{C}\{^1\text{H}\}$ NMR spectrum of $\text{anthH}_4^{\text{SiPr}_3}\text{-NMe}_2$ in CDCl_3	S14
Figure S17. ^1H NMR spectrum of $\text{anthZr}_2^{\text{SiPr}_3}\text{-NMe}_2$ in C_6D_6	S14
Figure S18. $^{13}\text{C}\{^1\text{H}\}$ NMR spectrum of $\text{anthZr}_2^{\text{SiPr}_3}\text{-NMe}_2$ in C_6D_6	S15
Figure S19. ^1H NMR spectrum of $\text{anthH}_2^{\text{ArSiPr}_3}\text{-NMe}_2$ in CDCl_3	S15
Figure S20. $^{13}\text{C}\{^1\text{H}\}$ NMR spectrum of $\text{anthH}_2^{\text{ArSiPr}_3}\text{-NMe}_2$ in CDCl_3	S15
Figure S21. ^1H NMR spectrum of $\text{anthZr}_1^{\text{ArSiPr}_3}\text{-NMe}_2$ in C_6D_6	S16
Figure S22. $^{13}\text{C}\{^1\text{H}\}$ NMR spectrum of $\text{anthZr}_1^{\text{ArSiPr}_3}\text{-NMe}_2$ in C_6D_6	S16
Figure S23. $^{13}\text{C}\{^1\text{H}\}$ NMR spectra of 1-hexene homopolymers from $\text{Zr}_1^{\text{ArSiPr}_3}\text{-NMe}_2$, C_5 $\text{Zr}_2^{\text{SiPr}_3}\text{-NMe}_2$ and $\text{C}_2 \text{Zr}_2^{\text{SiPr}_3}\text{-NMe}_2$	S17
Figure S24. $^{13}\text{C}\{^1\text{H}\}$ NMR spectra of 1-hexene homopolymers from $\text{anthZr}_1^{\text{ArSiPr}_3}\text{-NMe}_2$ and $\text{anthZr}_2^{\text{SiPr}_3}\text{-NMe}_2$	S18
Figure S25. $^{13}\text{C}\{^1\text{H}\}$ NMR spectra of high temperature propylene homopolymers from $\text{Zr}_1^{\text{ArSiPr}_3}\text{-NMe}_2$, $\text{C}_5 \text{Zr}_2^{\text{SiPr}_3}\text{-NMe}_2$, $\text{C}_2 \text{Zr}_2^{\text{SiPr}_3}\text{-NMe}_2$, $\text{anthZr}_1^{\text{SiPr}_3}\text{-NMe}_2$, $\text{anthZr}_2^{\text{SiPr}_3}\text{-NMe}_2$.	S19
Figure S26. $^{13}\text{C}\{^1\text{H}\}$ NMR spectra of ethylene-propylene copolymers from $\text{Zr}_1^{\text{ArSiPr}_3}\text{-NMe}_2$, C_5 $\text{Zr}_2^{\text{SiPr}_3}\text{-NMe}_2$, $\text{C}_2 \text{Zr}_2^{\text{SiPr}_3}\text{-NMe}_2$, $\text{anthZr}_1^{\text{SiPr}_3}\text{-NMe}_2$, $\text{anthZr}_2^{\text{SiPr}_3}\text{-NMe}_2$.	S20
Figure S27. $^{13}\text{C}\{^1\text{H}\}$ NMR spectra of ethylene-propylene copolymers from $\text{pyZr}_1^{\text{ArSiPr}_3}$, $\text{pyZr}_2^{\text{SiPr}_3}$, $\text{pyZr}_1^{\text{ArSiPh}_3}$, $\text{pyZr}_2^{\text{SiPh}_3}$	S21
Figure S28. $^{13}\text{C}\{^1\text{H}\}$ NMR spectra of ethylene-hexene copolymers from $\text{Zr}_1^{\text{ArSiPr}_3}\text{-NMe}_2$, C_5 $\text{Zr}_2^{\text{SiPr}_3}\text{-NMe}_2$, $\text{C}_2 \text{Zr}_2^{\text{SiPr}_3}\text{-NMe}_2$, $\text{anthZr}_1^{\text{SiPr}_3}\text{-NMe}_2$, $\text{anthZr}_2^{\text{SiPr}_3}\text{-NMe}_2$.	S22
Figure S29. $^{13}\text{C}\{^1\text{H}\}$ NMR spectra of ethylene-hexene copolymers from $\text{pyZr}_1^{\text{ArSiPr}_3}$, $\text{pyZr}_2^{\text{SiPr}_3}$, $\text{pyZr}_1^{\text{ArSiPh}_3}$, $\text{pyZr}_2^{\text{SiPh}_3}$.	S23
Figure S30. $^{13}\text{C}\{^1\text{H}\}$ NMR spectra of ethylene-tetradecene copolymers from $\text{Zr}_1^{\text{ArSiPr}_3}\text{-NMe}_2$, $\text{C}_5 \text{Zr}_2^{\text{SiPr}_3}\text{-NMe}_2$, $\text{C}_2 \text{Zr}_2^{\text{SiPr}_3}\text{-NMe}_2$, $\text{anthZr}_1^{\text{SiPr}_3}\text{-NMe}_2$, $\text{anthZr}_2^{\text{SiPr}_3}\text{-NMe}_2$.	S24
<i>Polymer Tables</i>	S25
Table S1. Ethylene-propylene copolymerization by $(^t\text{BuSi}^i\text{Pr}_3\text{-NMe}_2)\text{Zr}$	S25
Table S2. 1-Hexene and Propylene Homopolymerization	S26
Table S3. 1-Hexene and 1-Tetradecene Copolymerization.	S27
<i>Crystallographic Information</i>	S28
Refinement Details	S28
Table S4. Crystal and refinement data for $\text{Zr}_1^{\text{ArSiPr}_3}\text{-NMe}_2$, $\text{Zr}_2^{\text{SiPr}_3}\text{-NMe}_2$, and $\text{anthZr}_2^{\text{SiPr}_3}\text{-NMe}_2$	S29
Figure S31. Structural drawing of $\text{Zr}_1^{\text{ArSiPr}_3}\text{-NMe}_2$	S30
Figure S32. Structural drawing of $\text{Zr}_2^{\text{SiPr}_3}\text{-NMe}_2$	S31
Figure S33. Structural drawing of $\text{anthZr}_2^{\text{SiPr}_3}\text{-NMe}_2$	S32
<i>References</i>	S33

Experimental Details

1-bromo-2,3,4,5,6-pentamethylbenzene¹, 9-bromo,10-methylantracene², 2-Bromo-4-*tert*-butyl-1-(methoxymethoxy)benzene (**9**)³, **tBu10**⁴, 2,6-dibromo-4-*tert*-butylphenol⁵ and compounds **4** and **10**⁶ were prepared according to literature procedure.

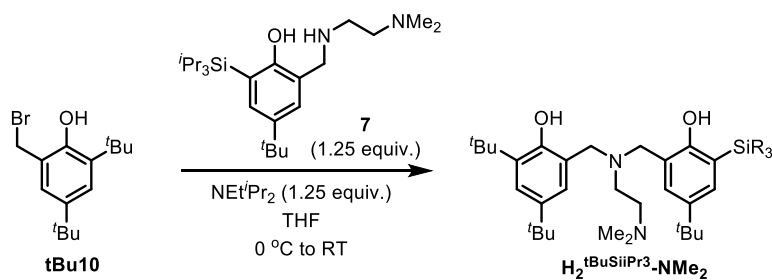
Synthesis of tetrabenzylzirconium.

In the glovebox, a round bottom was charged with a stirbar, 60 mL Et₂O, and benzylmagnesium chloride (126 mL, 1.9 M in Et₂O, 126 mmol, 4.2 equiv.) and frozen in the cold well. ZrCl₄ (7.043 g, 30.22 mmol, 1 equiv.) was added to the top of the thawing solution in 3 portions. The resulting yellow suspension was stirred 1 h, warming, then capped with a septum and stored at -35 °C without stirring. After 8 h, volatiles were removed and the residue was extracted with toluene and filtered over Celite. Concentration of the filtrate resulted in the formation of microcrystalline orange solids which were suspended in Et₂O, collected by filtration, and dried under vacuum to afford the desired product (8.89 g, 19.5 mmol, 65 %).



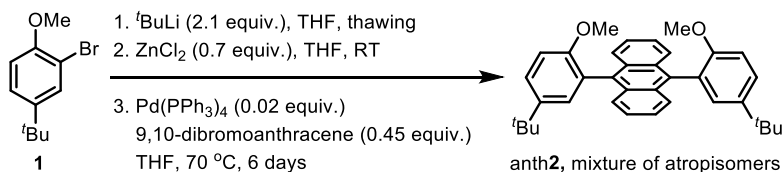
Synthesis of compounds **5**, **6**, and **15** were prepared according to the literature⁷.

Synthesis of compound 7. To a solution of **6** (4.530 g, 13.54 mmol, 1 equiv.) in methanol (54 mL) N,N-dimethylethylenediamine (1.8 mL, 16.5 mmol, 1.2 equiv.) was added and the reaction heated to 70 °C for 12 h. Volatiles were removed and the residue was taken up in methanol (54 mL) and NaBH₄ (2.2043 g, 58.27 mmol, 4.3 equiv.) was added in several portions, then the reaction stirred 4 h. The resulting colorless solution was concentrated and HCl (2N) added to quench. 1 M NaOH was added in small portions to bring to pH~7 and the white suspension was extracted thrice with DCM. Combined organics were washed with water, dried with MgSO₄, filtered, and evaporated to afford the product as a purple oil which was used without further purification (4.600 g, 11.31 mmol, 84 %). ¹H NMR (500 MHz, CDCl₃) δ 7.31 (d, *J* = 2.5 Hz, 1H), 6.97 (d, *J* = 2.5 Hz, 1H), 3.96 (s, 2H), 2.73 (m, 2H), 2.48 (m, 2H), 2.27 (s, 6H), 1.50 (m, 3H), 1.28 (s, 9H), 1.09 (d, *J* = 7.63 Hz, 18H). Note: ¹H NMR resonances corresponding to the N-H and O-H are not observed, likely due to exchange with trace water. ¹³C NMR (126 MHz, CDCl₃) δ 161.13 (Ar), 140.11 (Ar), 133.12 (Ar), 126.29 (Ar), 120.56 (Ar), 120.48 (Ar), 58.20 (ArCH₂), 45.41 (CH₂), 45.31 (CH₂), 33.90 (C(CH₃)₃), 31.66 (C(CH₃)₃), 19.01 (Si(CH₃)₂), 11.83 (Si(CH₃)₃). HRMS (FAB⁺) calcd for C₂₄H₄₇N₂OSi (M+H)⁺: 407.3458. Found: 407.3476.



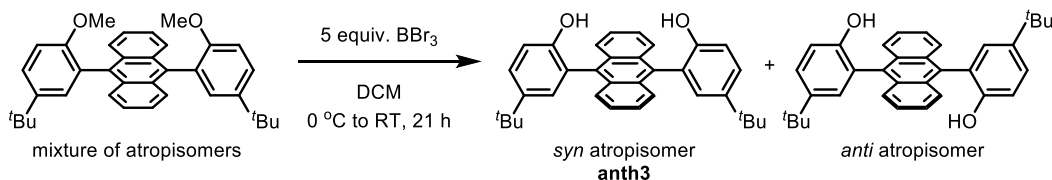
Synthesis of $\text{H}_2^{\text{tBuSiPr}_3}\text{-NMe}_2$. To a solution of **7** (1.173 g, 2.844 mmol, 1 equiv.) and NEt^iPr_2 (0.51 mL, 2.9 mmol, 1.25 equiv.) in THF (86 mL) at 0 °C, **tBu10** (0.577 g, 1.93 mmol, 1 equiv.) in THF (38 mL) was added in 2 mL portions. The reaction was stirred, warming over 3 h then volatiles removed under reduced pressure. The residue was taken up in DCM and washed with K_2CO_3 (2x) and brine. The combined organics were dried with MgSO_4 , filtered, and evaporated to afford the crude product which was further purified by column chromatography in 10:1 Hexanes:EtOAc (v/v) (1.021 g, 1.633 mmol, 85%). ^1H NMR (500 MHz, CDCl_3) δ 10.36 (br s, 1H, OH), 9.43 (br s, 1H, OH), 7.38 (d, 1H, ArH), 7.21 (d, 1H, ArH), 7.06 (d, 1H, ArH), 6.90 (d, 1H, ArH), 3.73 (s, 2H, ArCH₂), 3.57 (s, 2H, ArCH₂), 2.60 (br m, 4H, CH₂), 2.32 (s, 6H, N(CH₃)₂), 1.53 (sep, 3H, CH(CH₃)₂), 1.37 (s, 9H, C(CH₃)₃), 1.32 (s, 9H, C(CH₃)₃), 1.30 (s, 9H, C(CH₃)₃), 1.15 (d, 18H, CH(CH₃)₂). ^{13}C NMR (126 MHz, CDCl_3) δ 160.29, 153.32, 140.50, 139.85, 135.83, 134.29, 128.61, 124.45, 123.26, 121.68, 121.38, 120.14, 58.09, 56.14, 56.06, 49.23, 44.93, 35.00, 34.25, 33.97, 31.85, 30.49, 29.61, 19.27, 11.96. HRMS (FAB+) calcd for $\text{C}_{39}\text{H}_{69}\text{O}_2\text{N}_2\text{Si}$ (M+H)⁺: 625.5128. Found: 625.5107.

Synthesis of $\text{Zr}_1^{\text{tBuSiPr}_3}\text{-NMe}_2$. A 20 mL scintillation vial was charged with a stirbar, zirconium tetrabenzyl (62.0 mg, 0.136 mmol, 1.0 equiv.), and toluene (1.5 mL). The proligand (84.7 mg, 0.136 mmol, 1.0 equiv.) in toluene (2) was added over several minutes then the reaction stirred for 3 hours in the dark. Volatiles were removed *en vacuo* and the residue fractionated between pentane (6 mL) and ether (6 mL). The desired complex was isolated in as a bright yellow solid from the ether fraction (68.8 mg, 0.0767 mmol, 56 %). ^1H NMR (500 MHz, C_6D_6) δ 7.76 (d, 1H, ArH), 7.67 (d, 2H, ArH), 7.61 (d, 1H, ArH), 7.39 (t, 2H, ArH), 7.09 (d, 1H, ArH), 7.03 (t, 1H, ArH), 6.98 (d, 2H, ArH), 6.91 (d, 1H, ArH), 6.74 (t, 2H, ArH), 6.56 (t, 1H, ArH), 3.83 (d, 1H, ArCH₂), 3.04 (d, 1H, ArCH₂), 2.84 (d, 1H, ArCH₂), 2.78 (d, 1H, ArCH₂), 2.60 (d, 1H, ArCH₂), 2.58 – 2.51 (m, 2H, ArCH₂), 2.47 (d, 1H, ArCH₂), 2.19 (sep, 3H, CH(CH₃)₃), 1.83 (s, 9H), 1.54 (m, 13H), 1.47 (s, 4H), 1.42 – 1.34 (m, 29H). $^{13}\text{C}\{^1\text{H}\}$ NMR (126 MHz, C_6D_6) δ 164.71, 157.51, 148.85, 147.33, 140.93, 140.57, 136.21, 134.99, 126.87, 125.44, 124.49, 124.36, 124.28, 121.92, 121.76, 120.05, 68.83, 66.25, 64.92, 64.35, 59.72, 50.67, 36.54, 35.34, 34.03, 33.81, 31.52, 30.46, 19.95, 19.43, 12.92. Anal. Calcd $\text{C}_{53}\text{H}_{80}\text{N}_2\text{O}_2\text{SiZr}$: C, 71.00; H, 8.99; N, 3.12. Found: C, 70.92; H, 9.18; N, 3.20.



Synthesis of compound anth2. The teraryl compounds was synthesized via a Negishi coupling using the same general procedure as for the synthesis of **2**, *vide supra*. In the glove box, 2-bromo-4-*tert*-butylanisole (**1**) (19.72 g, 81.10 mmol, 1 equiv.) and 220 mL of THF were combined in a Schlenk tube and frozen in the cold well. $^t\text{BuLi}$ (100 mL, 170 mmol, 1.7 M in pentane, 2.1 equiv.) was added to the top of the frozen solution and the resulting solution allowed to stir, warming, for 1 h. ZnCl_2 (7.76 g, 56.9 mmol, 0.7 equiv.) was added in several portions to the solution with an additional 80 mL THF and the reaction stirred 1 h. 9,10-dibromoanthracene (12.402 g, 36.91 mmol, 0.45 equiv.), $\text{Pd}(\text{PPh}_3)_4$ (0.9412 g, 0.8145 mmol, 0.01 equiv.), and 80 mL THF were added at room temperature. The Schlenk tube was

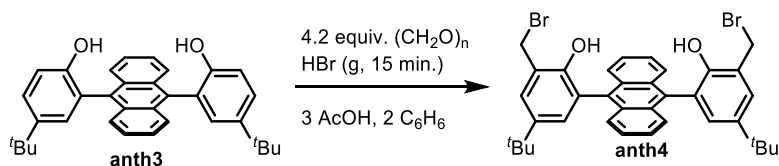
sealed, brought out of the glovebox and heated to 70 °C for 7 days. The vessel was cooled to room temperature and quenched by addition of water. The resulting chunky suspension was filtered over silica with excess dichloromethane and volatiles removed under reduced pressure. The residue was taken up in fresh dichloromethane and washed with water and brine, dried with MgSO₄, filtered, and evaporated to give a yellow solid. Precipitation from methanol afforded the desired product as a mixture of *syn* and *anti* atropisomers (10.89 g, 21.66 mmol, 59 %). ¹H NMR (300 MHz, CDCl₃) δ 7.66 (m, 4H, anth-*H*), 7.54 (dd, *J*=8.4, 2.5 Hz, 2H Ar-*H*), 7.39 (d, *J*=2.5 Hz, 2H, Ar-*H*), 7.31 (m, 4H, anth-*H*), 7.09 (d, *J*=8.7 Hz, 2H Ar-*H*), 3.64-3.49 (6H, OCH₃), 1.35-1.34 (18H, C(CH₃)₃). HRMS (FAB+) calcd for C₃₆H₃₈O₂: 502.2872. Found: 502.2889



Synthesis of compound anth3. An oven-dried 1 L Schlenk was assembled hot under flowing nitrogen and evacuated until cool to the touch. **Anth2** (3.606 g, 7.17 mmol, 1 equiv.) was added under positive N₂ flow and 180 mL dry DCM by cannula addition. The yellow solution was cooled to 0 °C with an ice-water bath and boron tribromide (3.5 mL, 36.3 mmol, 5 equiv.) added by syringe over the course of several minutes. The resulting brown solution was stirred, warming, for 21 h then quenched by slow addition of water with rapid stirring. Organics were washed with water (2x) and brine, then dried with MgSO₄, filtered, and evaporated. The crude mixture of atropisomers was purified by column chromatography in 5 hexanes: 1 EtOAc : 1/2 DCM (v/v/v) to afford the *anti* atropisomer (R_F ~ 0.5) further purified by precipitation from methanol (0.758 g, 1.59 mmol, 22 %) and *syn* atropisomer (R_F ~ 0.15, 1.25 g, 2.64 mmol, 37 %). HRMS (FAB+) calcd for C₃₄H₃₄O₂: 474.2559. Found: 474.2544.

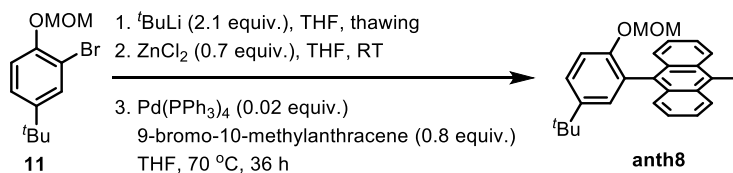
Anti Atropisomer: ¹H NMR (400 MHz, CDCl₃) δ 7.80-7.77 (m, 4H, anth*H*), 7.54-7.52 (dd, *J* = 2.1 Hz, *J* = 8.8 Hz, 2H, Ar*H*), 7.46-7.44 (m, 4 H, anth*H*), 7.35 (d, *J* = 2.1 Hz, 2H, Ar*H*), 7.13 (d, *J* = 8.5 Hz, 2H, Ar*H*), 4.48 (s, 2H, OH), 1.38 (s, 9H, C(CH₃)₃). ¹³C NMR (101 MHz, CDCl₃) δ 151.59, 143.77, 132.20, 130.96, 129.19, 126.92, 126.82, 126.45, 123.47, 34.47 (C(CH₃)₃), 31.81 (C(CH₃)₃).

Syn Atropisomer: ¹H NMR (500 MHz, CDCl₃) δ 7.81-7.79 (m, 4H, anth*H*), 7.55-7.53 (dd, *J* = 2.4 Hz, *J* = 8.6 Hz, 4H, Ar*H*), 7.48-7.46 (m, 4H, anth*H*), 7.33 (d, *J* = 2.4 Hz, 2H, Ar*H*), 7.15 (d, *J* = 8.6 Hz, 2H, Ar*H*), 4.55 (s, 2H, OH), 1.38 (s, 9H, C(CH₃)₃). ¹³C NMR (126 MHz, CDCl₃) δ 151.44, 143.65, 132.26, 130.79, 129.22, 126.78, 126.69, 126.30, 123.35, 115.24, 34.32 (C(CH₃)₃), 31.65 (C(CH₃)₃).

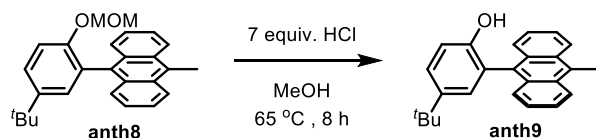


Synthesis of compound anth4. A Schlenk flask was charged with a stirbar, **anth3** (3.734 g, 7.867 mmol, 1 equiv.), paraformaldehyde (0.994 g, 33.1 mmol, 4.2 equiv.), 24 mL glacial acetic acid, and 12 mL benzene. Anhydrous HBr (g) was bubbled through the resulting suspension, with rapid stirring, for 15 min. (Note: excess HBr (g) was bubbled through water and 1 M NaOH to neutralize.) The resulting brown solution was stirred 4 h, then diluted with hexanes and dichloromethane (ca. 2:1 v/v) and washed with water (2x) and brine, dried with MgSO₄, filtered, and evaporated. Precipitation from hexanes afforded the desired product as an emerald green solid (3.38 g, 5.11 mmol, 65 %). ¹H NMR (400 MHz, CDCl₃) δ 7.76-7.73 (m, 4 H, anth*H*), 7.56 (d, 2 H, Ar*H*), 7.48-7.46 (m, 4 H, anth*H*), 7.30 (d, 2 H, Ar*H*), 4.85 (bs, 2 H, OH), 4.74 (s, 4 H, CH₂Br), 1.36 (s, 18 H, C(CH₃)₃). ¹³C {¹H} NMR (101 MHz, CDCl₃) δ

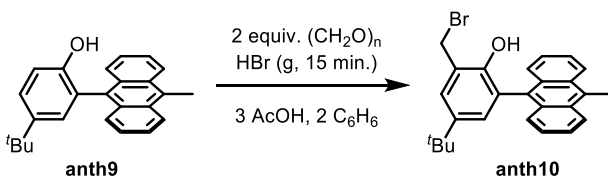
149.79, 143.74, 131.76, 130.75, 130.08, 128.03, 126.61, 126.53, 124.11, 123.96, 34.35, 31.55, 29.87. HRMS (FAB+) calcd for C₃₆H₃₆Br₂O₂: 660.1062. Found: 660.1069



Synthesis of compound anth8. In the glove box, **11** (4.592 g, 16.81 mmol, 1 equiv.) and 30 mL THF were combined in a Schlenk tube and frozen in the cold well. ^tBuLi (21.0 mL, 35.7 mmol, 1.7 M in pentane, 2.1 equiv.) was added to the top of the frozen solution and the resulting solution allowed to stir, warming, for 30 min. ZnCl₂ (1.708 g, 12.53 mmol, 0.7 equiv.) was added in several portions to the solution with an additional 20 mL THF and the reaction stirred 1 h. 9-bromo-10-methylantracene (3.671 g, 13.54 mmol, 0.8 equiv.), Pd(PPh₃)₄ (0.251 g, 0.217 mmol, 0.01 equiv.), and 20 mL THF were added at room temperature. The Schlenk tube was sealed, brought out of the glovebox and heated to 70 °C for 36 h. The reaction was cooled to room temperature and quenched by addition of water. The resulting chunky suspension was filtered over silica with excess dichloromethane and volatiles removed under reduced pressure. The residue was taken up in fresh dichloromethane and washed with water and brine, dried with MgSO₄, filtered, and evaporated to give a yellow solid. Precipitation from methanol afforded the desired product as a yellow solid in ca. 85 % NMR purity (3.38 g, 8.78 mmol, 65 %). ¹H NMR (300 MHz, CDCl₃) δ 8.35 (d, *J*=8.7 Hz, 2H, anth*H*), 7.66 (d, *J*=8.6 Hz, 2H, anth*H*), 7.52-7.48 (m, 3H, Ar*H*), 7.37-7.28 (m, 6H, Ar*H*), 4.87 (s, 2H, OCH₂OCH₃), 3.18 (s, 3H, anthCH₃), 3.03 (s, 3H, OCH₂OCH₃), 1.33 (s, C(CH₃)₃). ¹³C NMR (101 MHz, CDCl₃) δ 153.22, 144.74, 132.98, 130.29, 130.15, 129.82, 128.16, 127.71, 125.73, 124.94, 124.73, 124.65, 114.61, 94.22, 55.76, 34.31, 31.58. HRMS (FAB+) calcd for C₂₇H₂₉O₂ (M+H)⁺: 385.2168. Found: 385.2155.

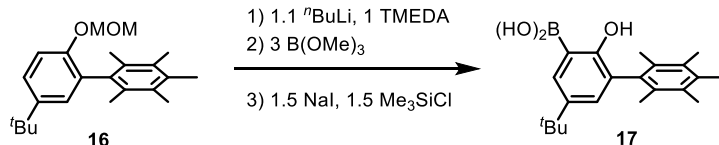


Synthesis of compound anth9. A round bottom was charged with a stirbar, **8** (2.97 g, 7.72 mmol, 1 equiv.), 62 mL MeOH, and concentrated HCl (10 mL, 14 equiv.) and heated to 65 °C for 8 h. The resulting suspension was concentrated then taken up in DCM and washed with water (2x) and brine, dried with MgSO₄, filtered, and evaporated. Purification by column chromatography in 10 % benzene in hexanes afforded the desired product as an off-white solid (1.43 g, 4.21 mmol, 55 %).

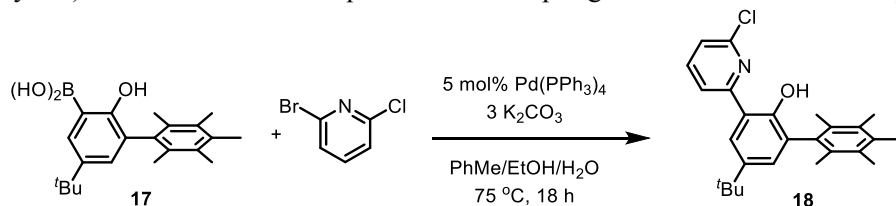


Synthesis of compound anth10. A Schlenk flask was charged with a stirbar, **anth9** (1.78 g, 5.23 mmol, 1 equiv.), paraformaldehyde (0.20 g, 6.5 mmol, 1.25 equiv.), 24 mL glacial acetic acid, and 12 mL benzene. Anhydrous HBr (g) was bubbled through the resulting suspension, with rapid stirring, for 15 min. (Note: excess HBr (g) was bubbled through water and 1 M NaOH to neutralize.) The resulting brown solution was stirred 4 h, then diluted with hexanes and dichloromethane and washed with water (2x) and brine,

dried with MgSO₄, filtered, and evaporated to afford the crude product as an emerald green solid (2.15 g, 4.96 mmol, 95 %) which was used for subsequent reactions without further purification.



Synthesis of compound 17 (10.0 g, 29 mmol, 1.0 equiv), *N,N,N',N'*-tetramethylethylenediamine (4.41 mL, 29 mmol, 1.0 equiv) and THF (80 mL) were added to a Schlenk tube under inert atmosphere and cooled down to $-78\text{ }^{\circ}\text{C}$ using a dry ice/acetone cooling bath. *n*-Butyllithium (2.5 M solution in hexane, 12.9 mL, 32 mmol, 1.1 equiv) was added dropwise to the reaction solution and stirred while it warmed to room temperature for 4 h. The resultant orange red solution was re-cooled at $-78\text{ }^{\circ}\text{C}$ and trimethyl borate (9.70 mL, 87 mmol, 3.0 equiv) was added dropwise to the reaction mixture. After 30 min. of stirring at $-78\text{ }^{\circ}\text{C}$, the reaction mixture was allowed to warm to room temperature and stirred for 15 h. A saturated solution of NH₄Cl (aq) (30 mL) was added to quench the reaction. Crude product was extracted with diethyl ether (3 times) and washed with brine (2 times), dried over anhydrous MgSO₄, filtered, and concentrated to dryness. The residue was dissolved in THF (80 mL) and NaI (6.52 g, 43.5 mmol, 1.5 equiv), trimethylsilylchloride (5.52 mL, 43.5 mmol, 1.5 equiv) was added to the reaction solution. The resulting solution was stirred at room temperature for 15 h. The product was extracted with diethyl ether (3 times) and washed with water and brine, dried over MgSO₄, filtered, and concentrated *in vacuo*. Crude product was precipitated from MeOH and dried under *vacuo*. This crude slightly yellow powder (7.50 g, 20 mmol, 75% yield) was used for the subsequent Suzuki coupling reaction without further purification.



Synthesis of compound 18. A mixture of boronic acid, **17** (2 g, 6 mmol), 2-bromo-6-chloropyridine (1.12 g, 5.87 mmol), and potassium carbonate (2.43 g, 17.6 mmol) were dissolved in a mixture of toluene (40 mL), ethanol (13 mL) and water (13 mL). The reaction mixture was degassed via three freeze-pump-thaw cycles and then, tetrakis(triphenylphosphine)palladium(0) (0.399 g, 0.294 mmol) was added to the reaction mixture and the resulting yellow solution was stirred at $75\text{ }^{\circ}\text{C}$ for 24 h. After the reaction completed, the organic layer was separated and the aqueous layer was extracted with ethyl acetate. The combined organic layer was washed with brine, dried over anhydrous MgSO₄, filtered, and concentrated to dryness. Purification by flash column chromatography on silica gel using CH₂Cl₂–hexanes as the eluent (v/v = 3:1) gave slightly yellow solid 96% yield (2.3 g, 5.65 mmol). ¹H NMR (400 MHz, CDCl₃, 25 °C): δ 12.77 (s, 1H, OH), 7.91 (d, $J = 8.0$ Hz, 1H, CH of py), 7.81 (t, $J = 7.9$ Hz, 1H, CH of py), 7.77 (d, $J = 2.4$ Hz, 1H, CH of a phenol ring), 7.25–7.22 (m, 2H, CH of py and CH of a phenol ring), 2.31 (s, 3H, CH₃ of Ar), 2.29 (s, 6H, CH₃ of Ar), 2.04 (s, 6H, CH₃ of Ar), 1.37 (s, 9H, ^tBu). ¹³C NMR (101 MHz, CDCl₃, 25 °C): δ 159.3, 154.4, 148.3, 141.6, 139.9 (CH of py), 135.85, 134.4, 132.5, 132.1, 132.1, 131.6 (CH of py), 121.4 (CH of a phenol ring), 121.4₆ (CH of a phenol ring), 117.8, 117.1 (CH of py), 34.4 (C(CH₃)₃), 31.7 (CH₃ of ^tBu), 18.1 (CH₃ of Ar), 17.0 (CH₃ of Ar), 16.9 (CH₃ of Ar). HRMS (EI⁺) Calcd. For C₂₆H₃₁ClNO (M+H)⁺: 408.2094. Found: 408.2095.

NMR Characterization

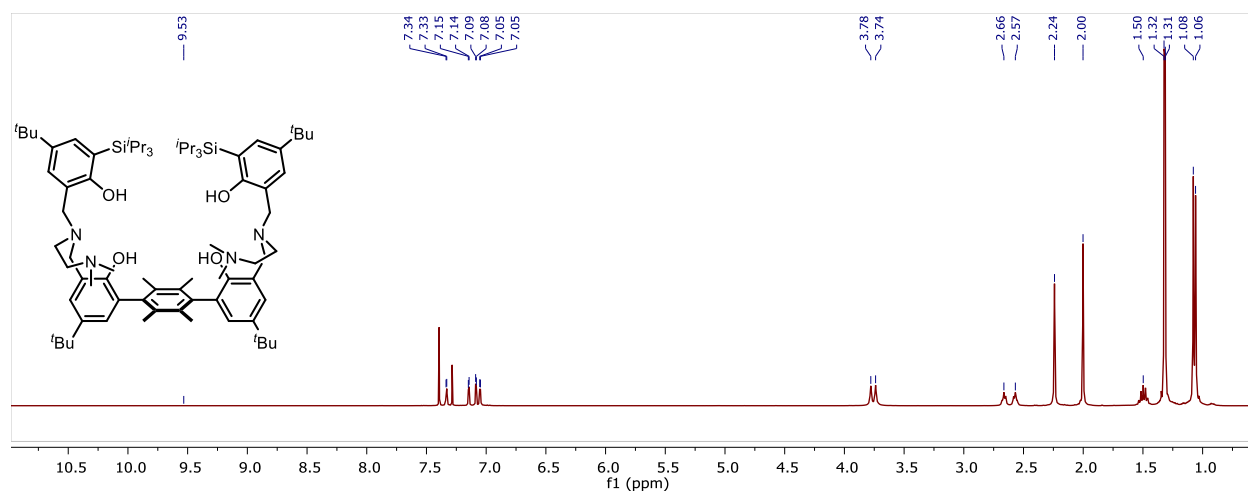


Figure S1. ^1H NMR spectrum of $\text{H}_4^{\text{SiPr}_3}\text{-NMe}_2$ in CDCl_3 .

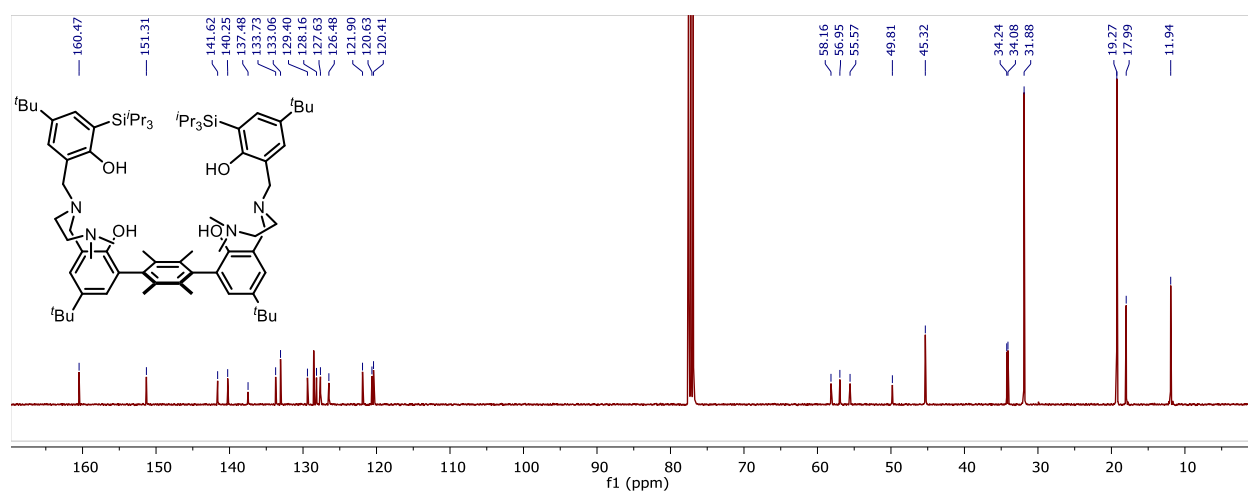


Figure S2. $^{13}\text{C}\{^1\text{H}\}$ NMR spectrum of $\text{H}_4^{\text{SiPr}_3}\text{-NMe}_2$ in CDCl_3 .

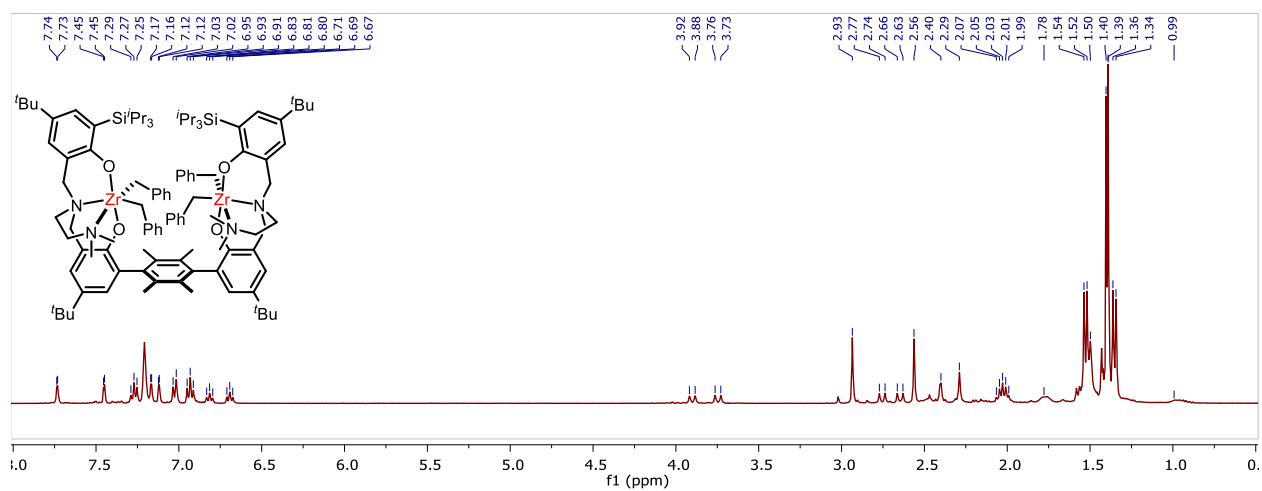


Figure S3. ^1H NMR spectrum of $\text{C}_s\text{Zr}_2^{\text{SiPr}_3}\text{-NMe}_2$ in C_6D_6 .

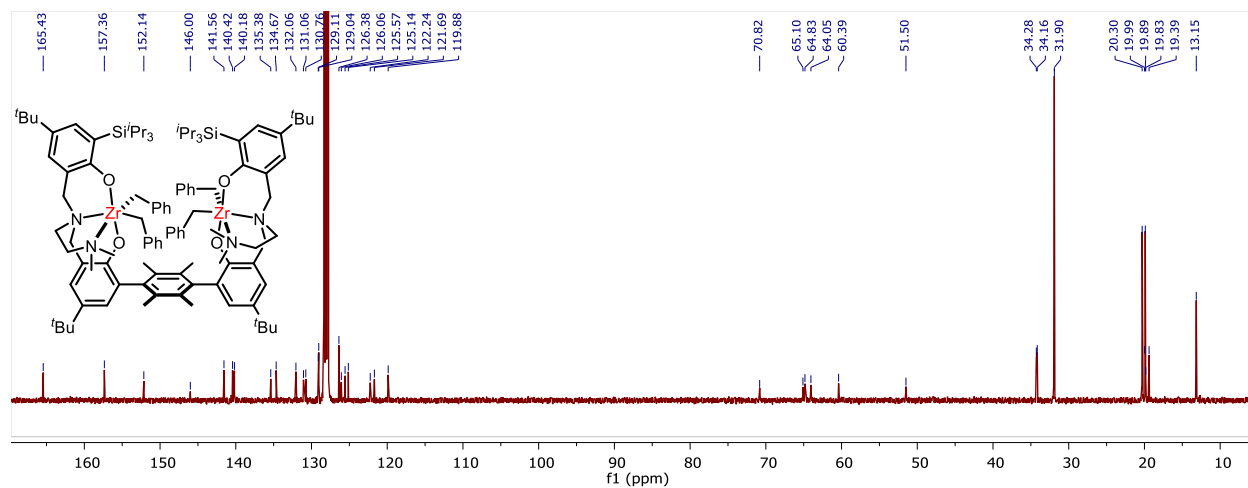


Figure S4. $^{13}C\{^1H\}$ NMR spectrum of $C_5 Zr_2^{SiPr^3}-NMe_2$ in C_6D_6 .

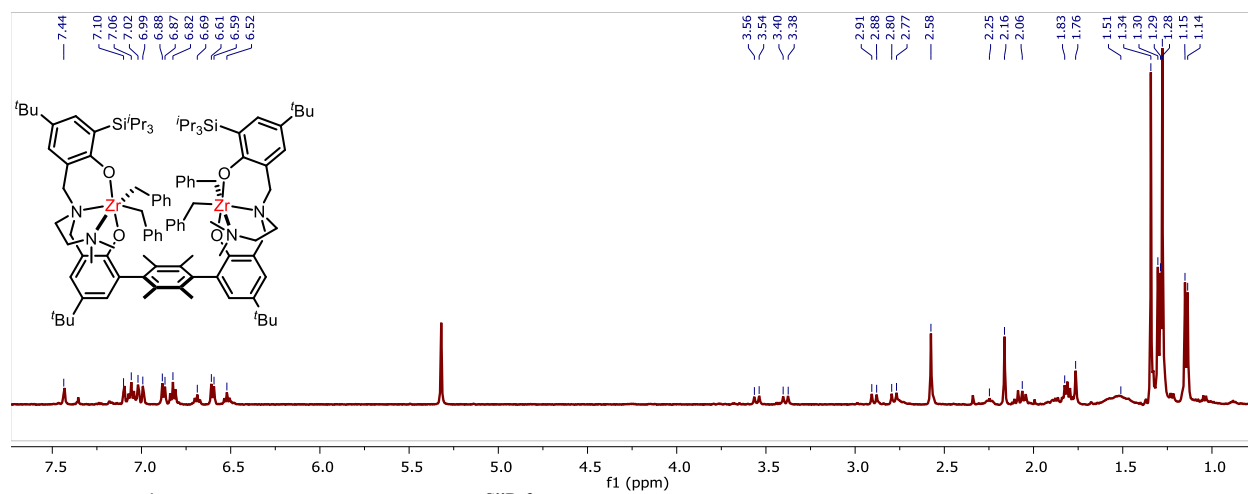


Figure S5. 1H NMR spectrum of $C_5 Zr_2^{SiPr^3}-NMe_2$ in CD_2Cl_2 .

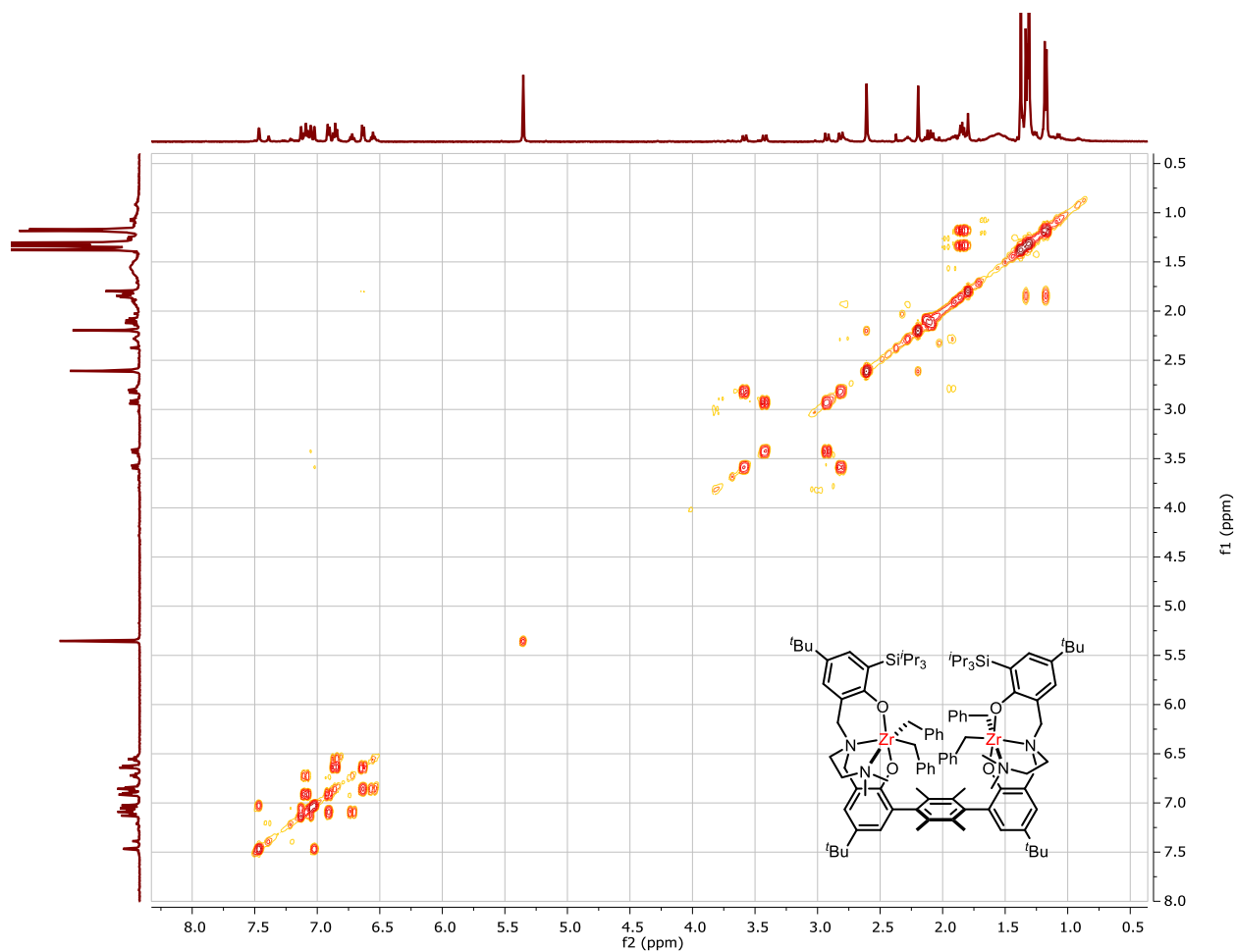


Figure S6. gCOSY spectrum of $C_5 Zr_2^{SiPr_3-NMe_2}$ in CD_2Cl_2 .

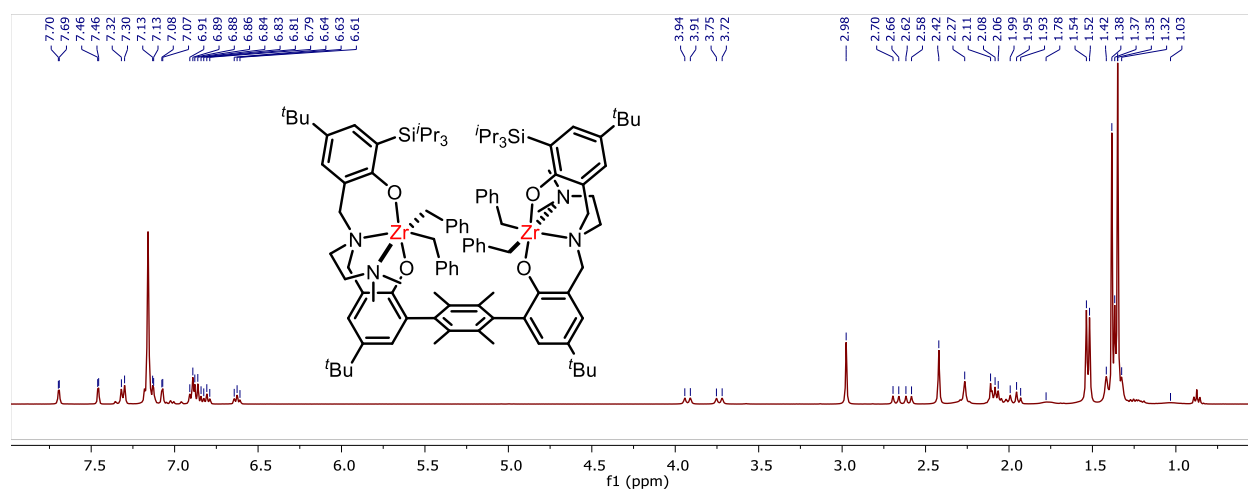


Figure S7. 1H NMR spectrum of $C_2 Zr_2^{SiPr_3-NMe_2}$ in C_6D_6 .

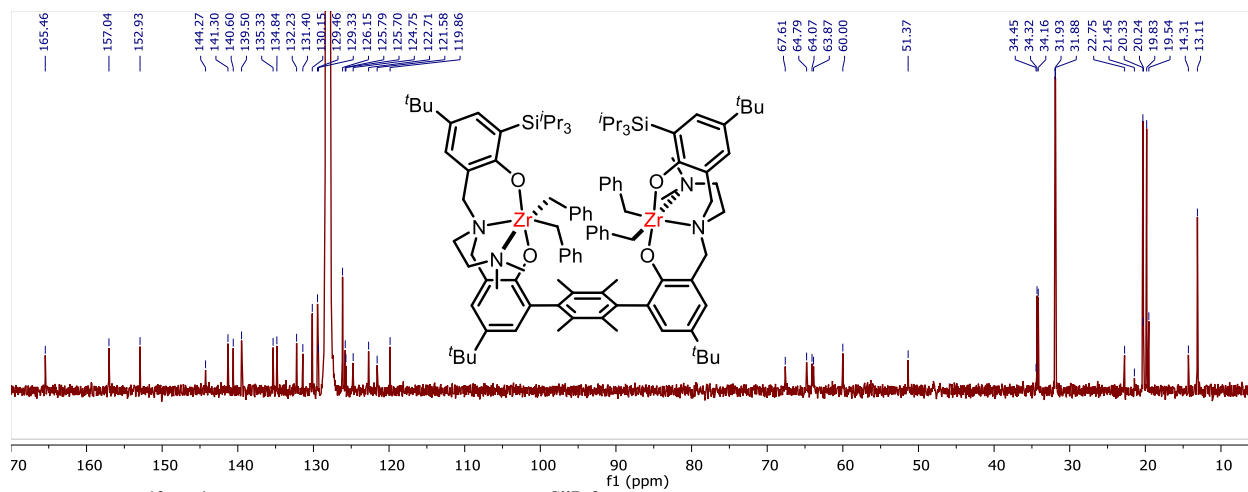


Figure S8. $^{13}C\{^1H\}$ NMR spectrum of $C_2 Zr_2^{SiPr^3}-NMe_2$ in C_6D_6 .

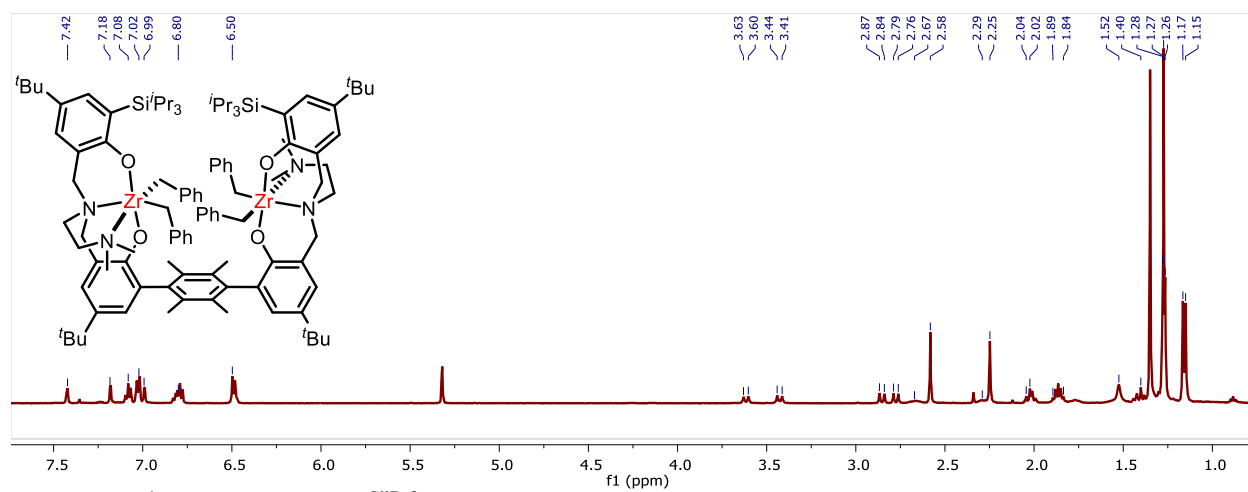


Figure S9. 1H NMR of $C_2 Zr_2^{SiPr^3}-NMe_2$ in CD_2Cl_2 .

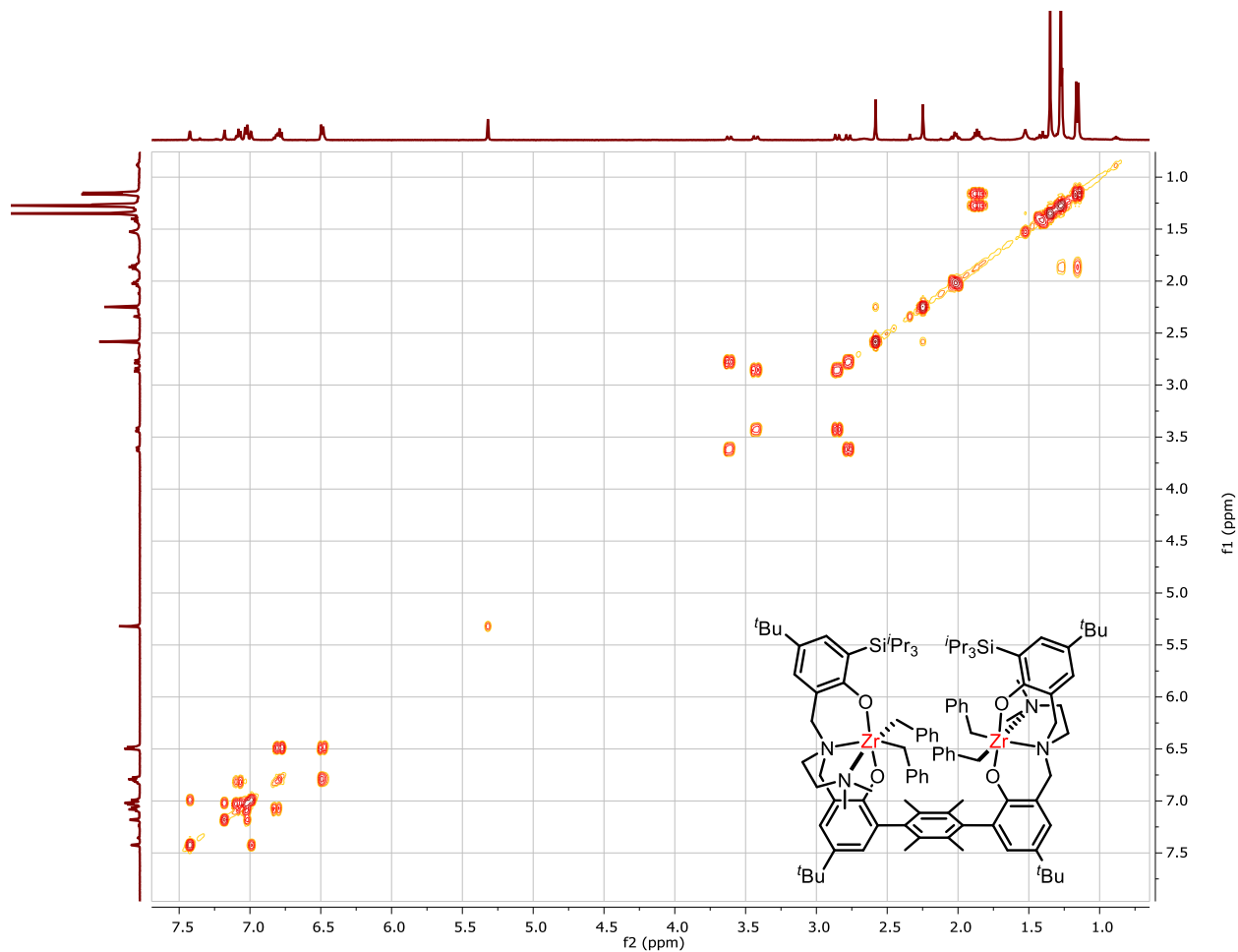


Figure S10. gCOSY of $C_2 Zr_2^{SiPr_3}-NMe_2$ in CD_2Cl_2 .

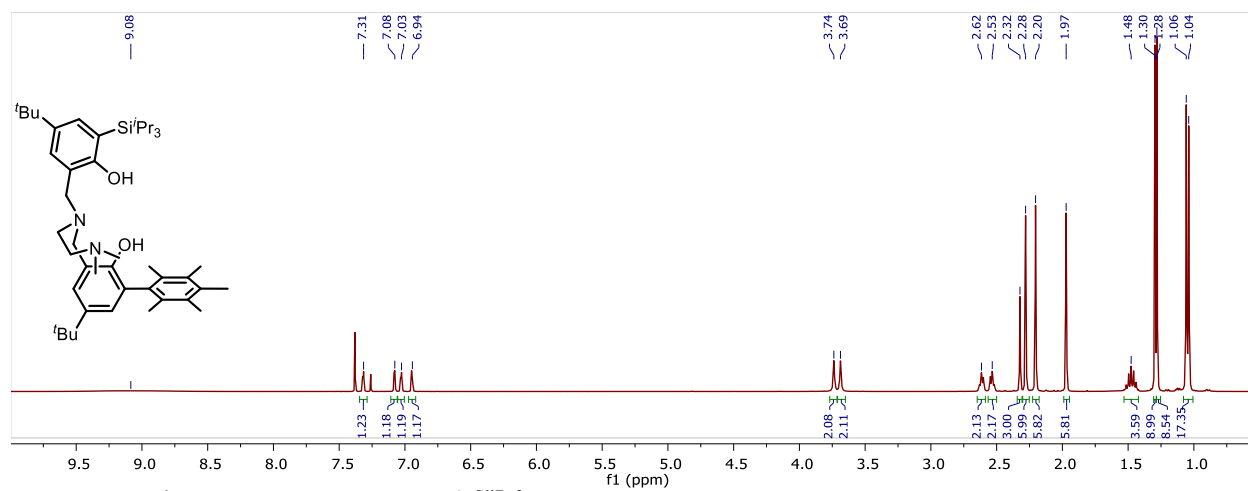


Figure S11. 1H NMR spectrum of $H_2^{ArSiPr_3}-NMe_2$ in $CDCl_3$.

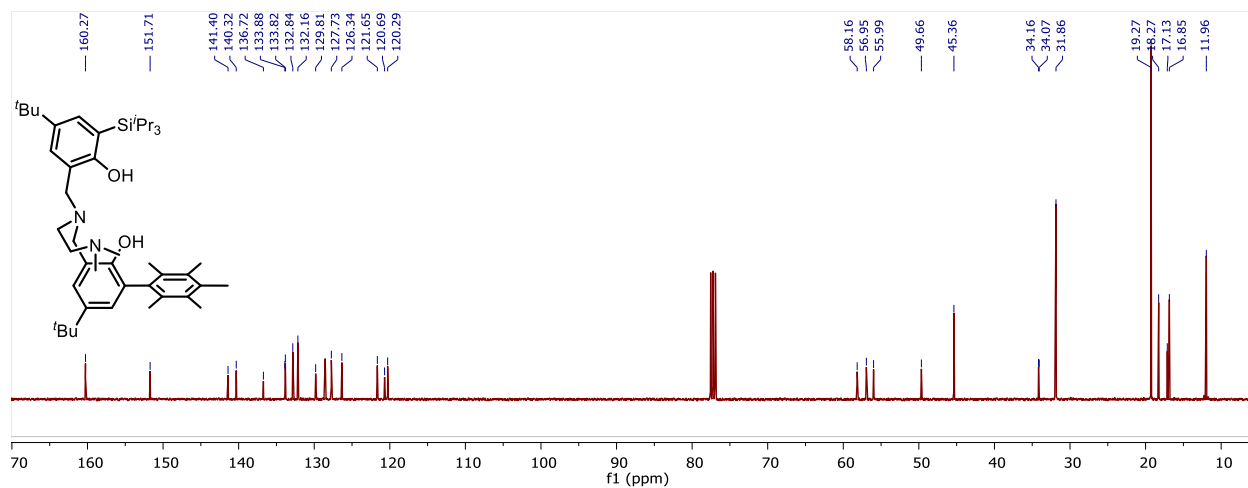


Figure S12. $^{13}\text{C}\{^1\text{H}\}$ NMR spectrum of $\text{H}_2\text{-ArSiPr}_3\text{-NMe}_2$ in CDCl_3 .

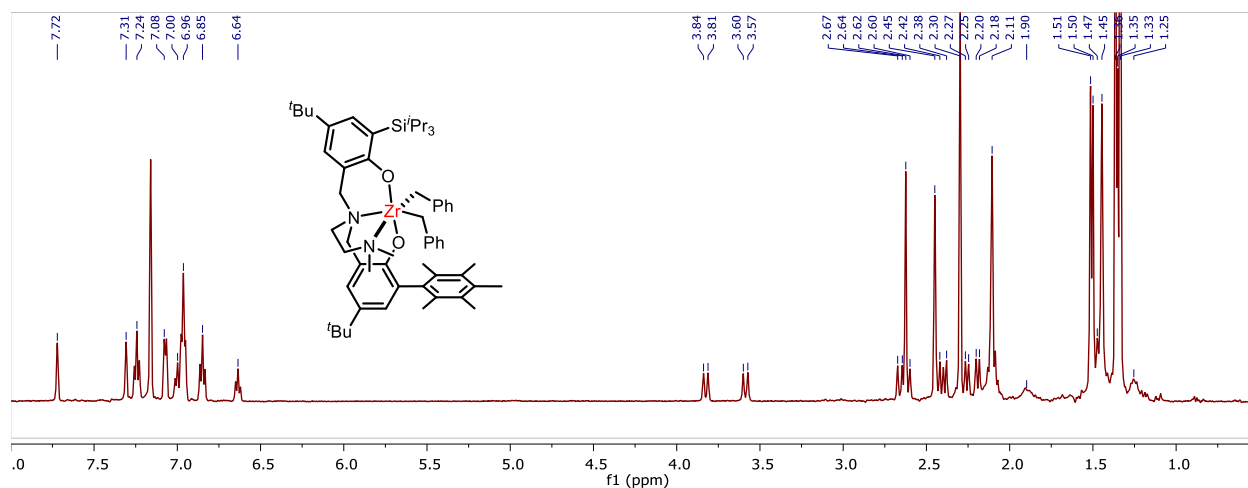


Figure S13. ^1H NMR spectrum of $\text{Zr}_1\text{-ArSiPr}_3\text{-NMe}_2$ in C_6D_6 .

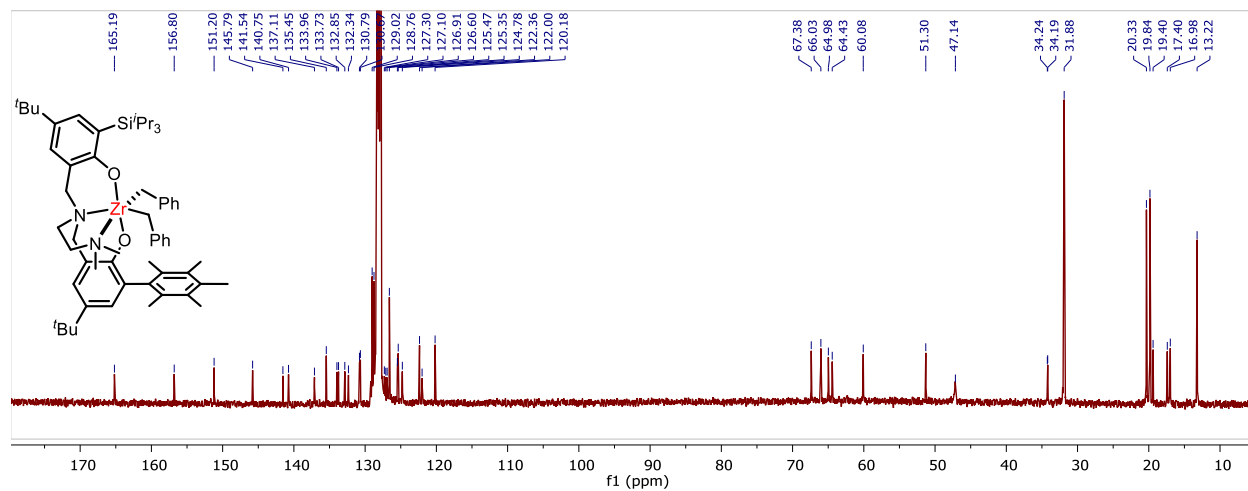
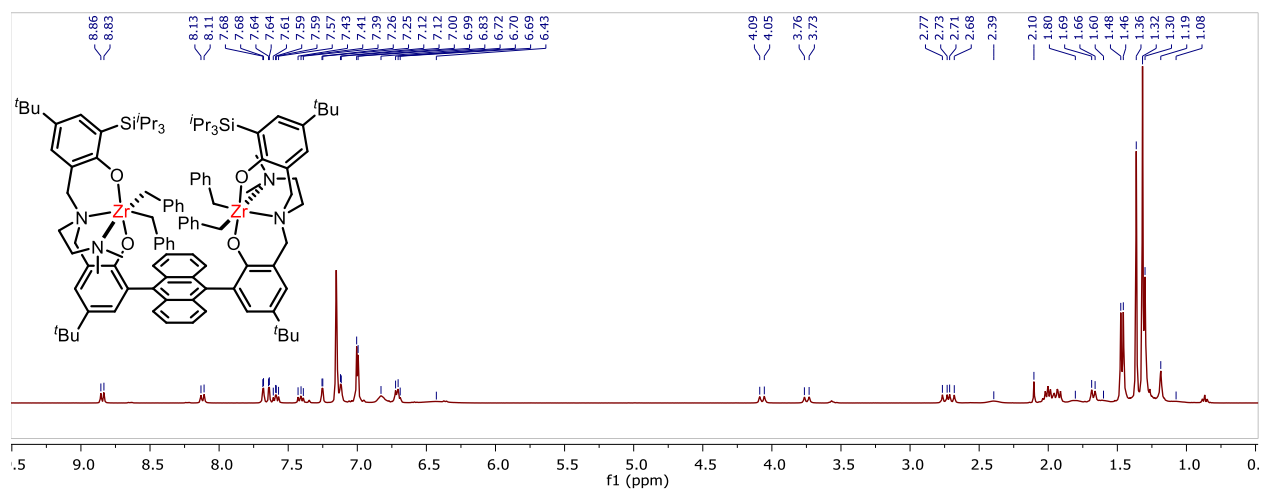
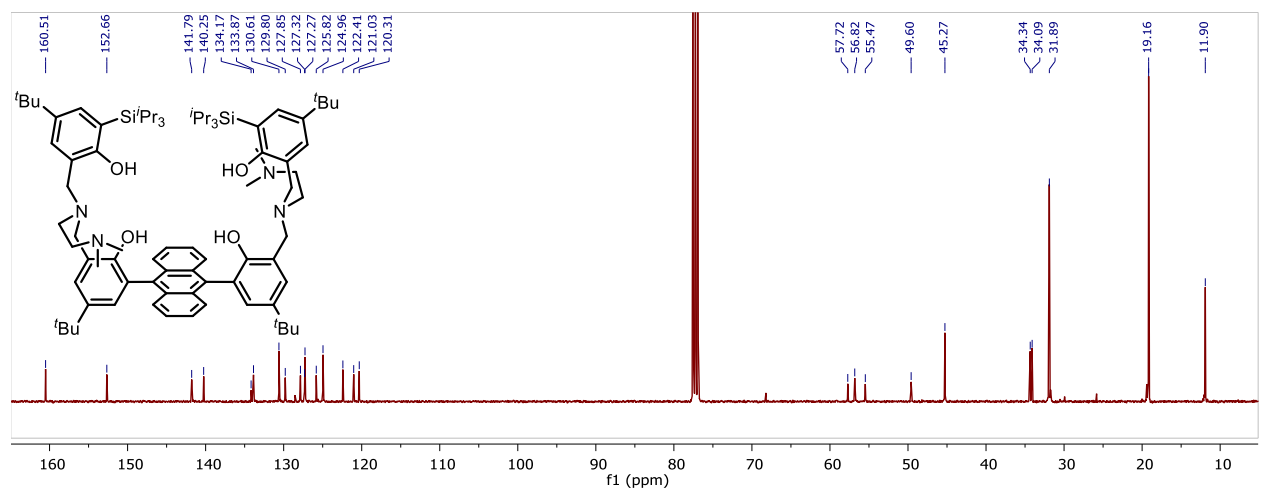
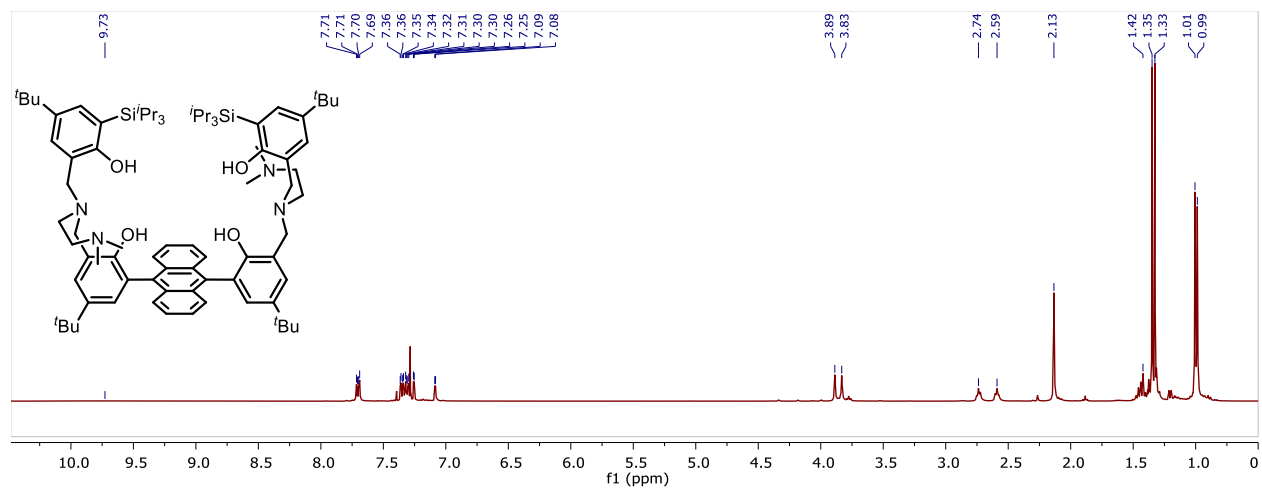


Figure S14. $^{13}\text{C}\{^1\text{H}\}$ NMR spectrum of $\text{Zr}_1\text{-ArSiPr}_3\text{-NMe}_2$ in C_6D_6 .



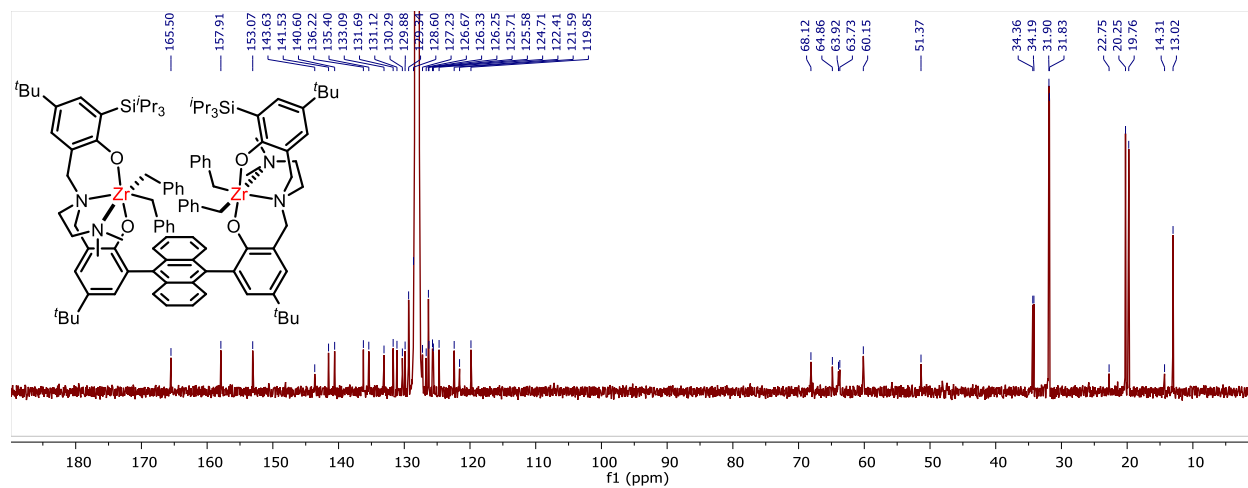


Figure S18. $^{13}\text{C}\{^1\text{H}\}$ NMR spectrum of $\text{anthZr}_2^{\text{Si}^i\text{Pr}_3}\text{-NMe}_2$ in C_6D_6 .

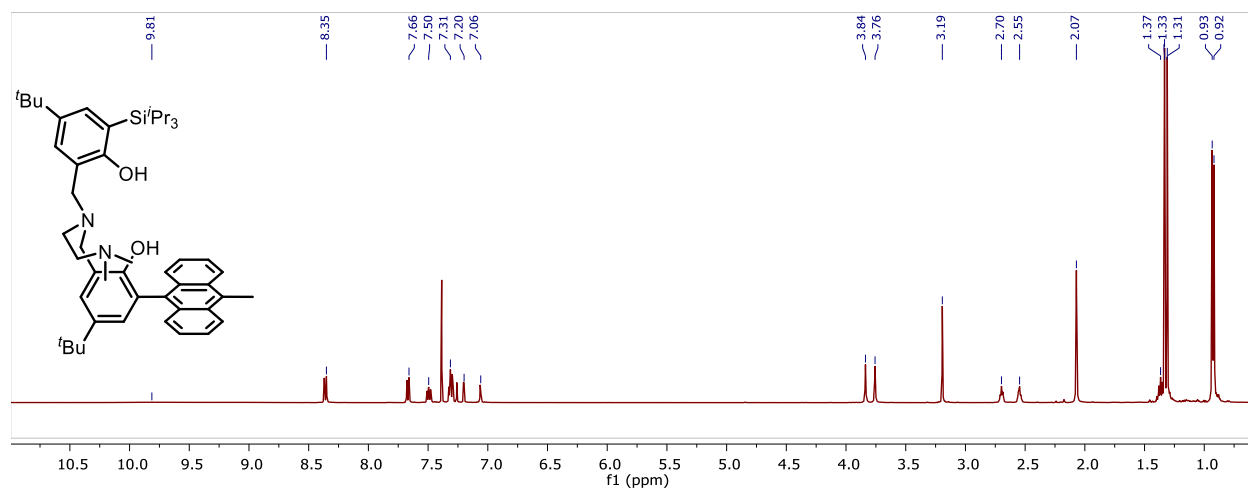


Figure S19. ^1H NMR spectrum of $\text{anthH}_2^{\text{ArSi}^i\text{Pr}_3}\text{-NMe}_2$ in CDCl_3 .

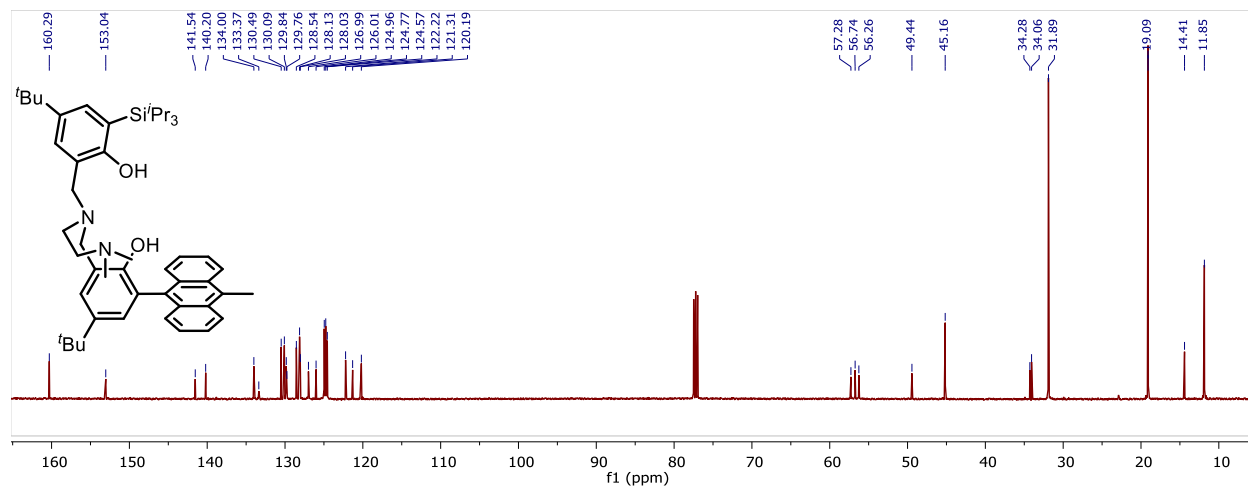


Figure S20. $^{13}\text{C}\{^1\text{H}\}$ NMR spectrum of $\text{anthH}_2^{\text{ArSi}^i\text{Pr}_3}\text{-NMe}_2$ in CDCl_3 .

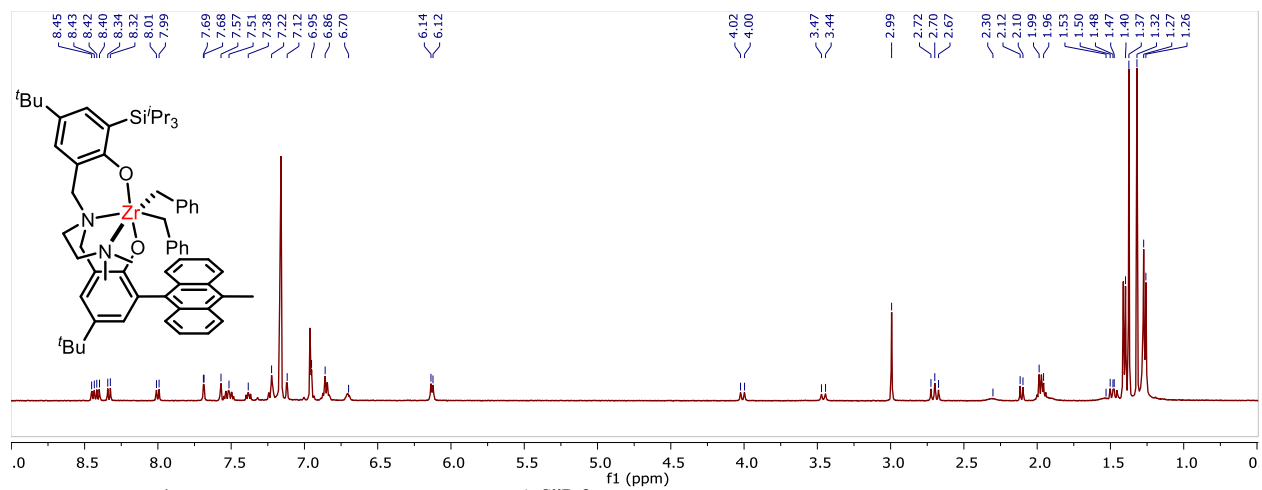


Figure S21. ^1H NMR spectrum of $\text{anthZr}_1^{\text{ArSiPr}_3}\text{-NMe}_2$ in C_6D_6 .

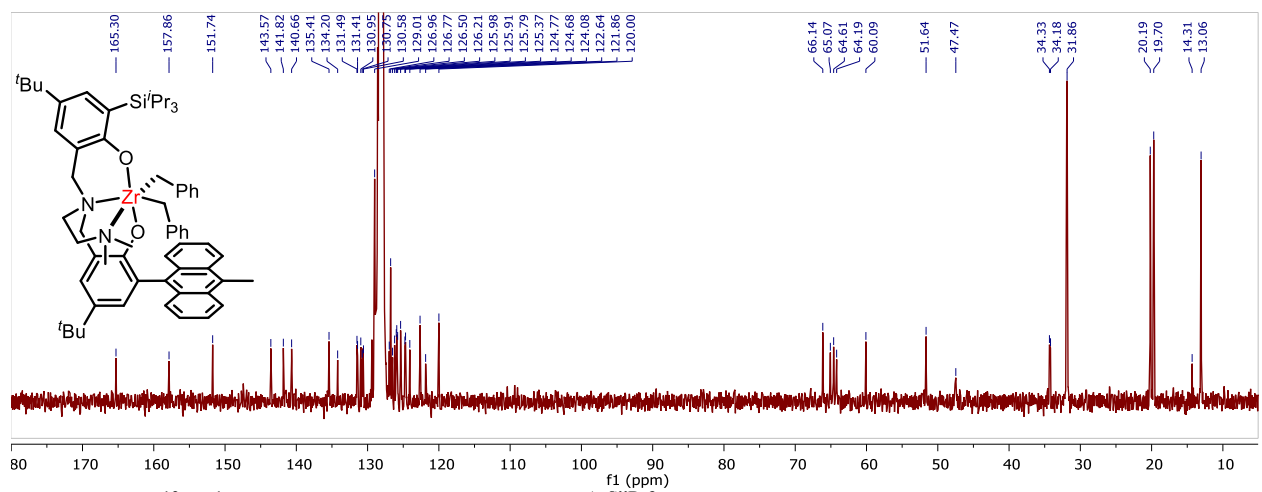


Figure S22. $^{13}\text{C}\{^1\text{H}\}$ NMR spectrum of $\text{anthZr}_1^{\text{ArSiPr}_3}\text{-NMe}_2$ in C_6D_6 .

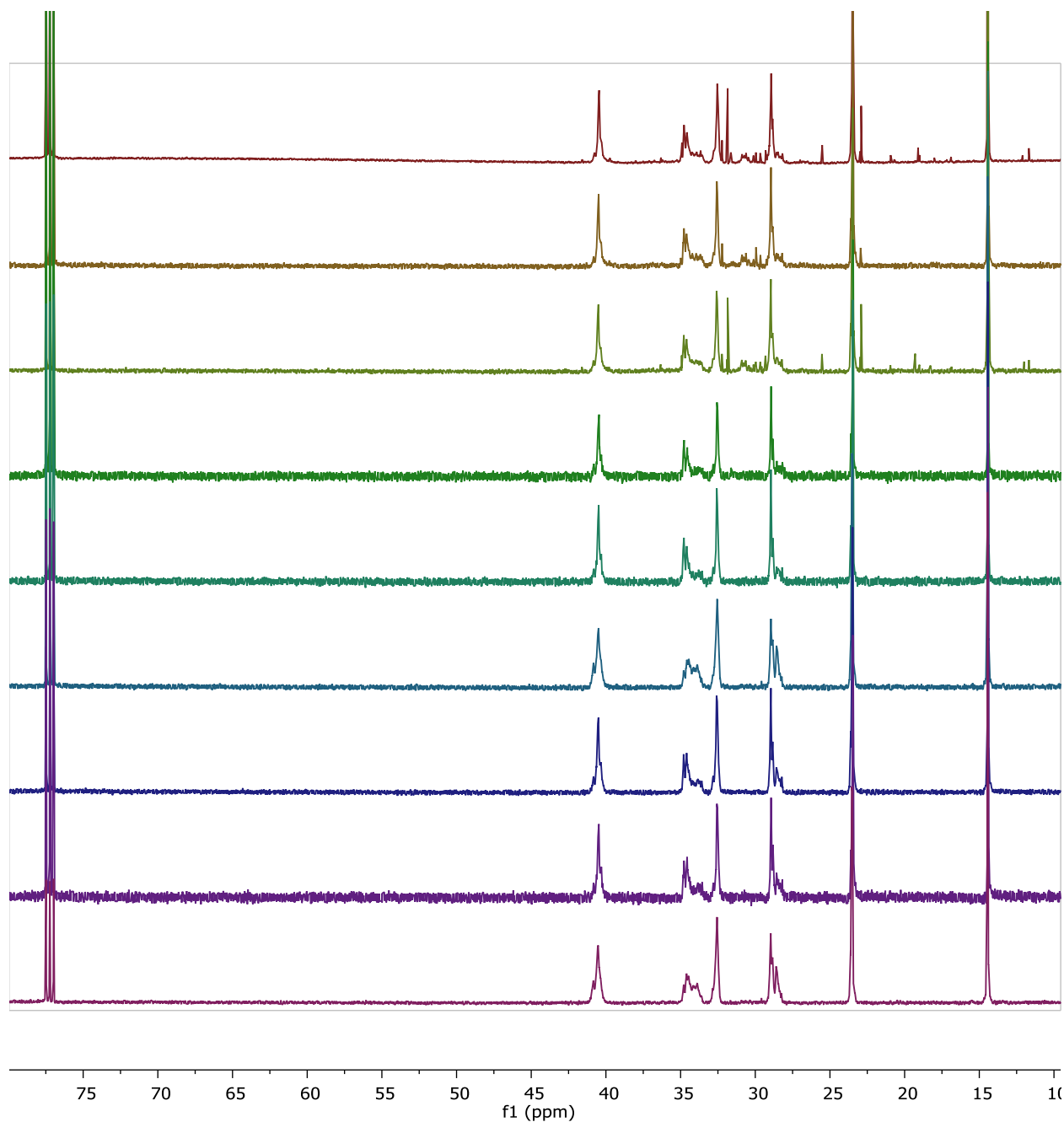


Figure S23. $^{13}\text{C}\{^1\text{H}\}$ NMR spectra in CDCl_3 at 25°C of 1-hexene homopolymers from (top to bottom) $\text{Zr}_1^{\text{ArSiPr}^3}\text{-NMe}_2$ with $[\text{CPh}_3][\text{B}(\text{C}_6\text{F}_5)_4]$, $[\text{HNMe}_2\text{Ph}][\text{B}(\text{C}_6\text{F}_5)_4]$, dried MAO; $\text{C}_8 \text{Zr}_2^{\text{SiPr}^3}\text{-NMe}_2$ with $[\text{CPh}_3][\text{B}(\text{C}_6\text{F}_5)_4]$, $[\text{HNMe}_2\text{Ph}][\text{B}(\text{C}_6\text{F}_5)_4]$, dried MAO; and $\text{C}_2 \text{Zr}_2^{\text{SiPr}^3}\text{-NMe}_2$ with $[\text{CPh}_3][\text{B}(\text{C}_6\text{F}_5)_4]$, $[\text{HNMe}_2\text{Ph}][\text{B}(\text{C}_6\text{F}_5)_4]$, dried MAO.

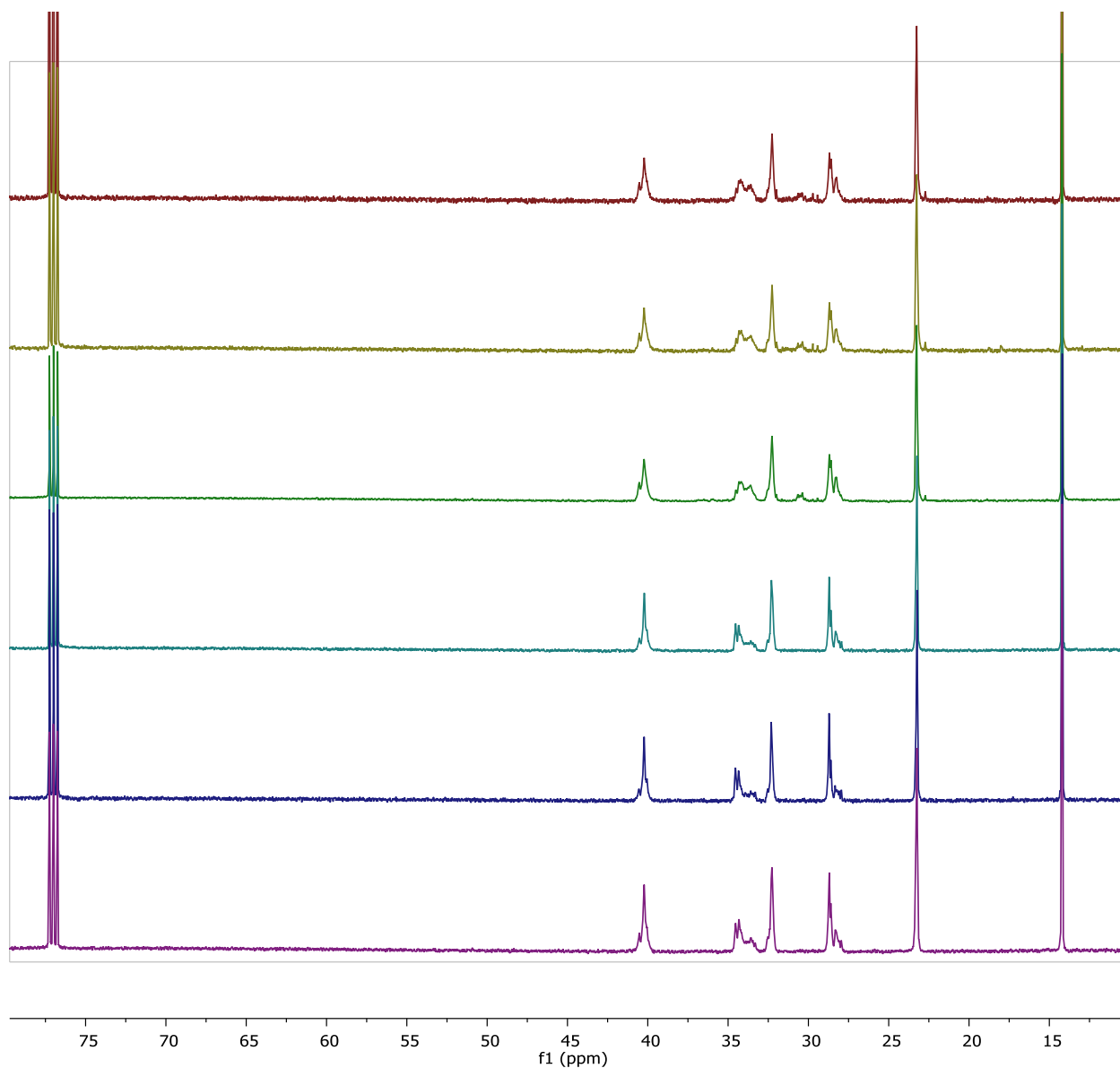


Figure S24. $^{13}\text{C}\{^1\text{H}\}$ NMR spectra in CDCl_3 at 25°C of 1-hexene homopolymers from (top to bottom) $\text{anthZr}_1^{\text{ArSiPr}^3}\text{-NMe}_2$ [CPh_3][$\text{B}(\text{C}_6\text{F}_5)_4$] (a), [HNMe_2Ph][$\text{B}(\text{C}_6\text{F}_5)_4$] (b), dried MAO (c) and C_2 $\text{anthZr}_2^{\text{SiPr}^3}\text{-NMe}_2$ [CPh_3][$\text{B}(\text{C}_6\text{F}_5)_4$] (d), [HNMe_2Ph][$\text{B}(\text{C}_6\text{F}_5)_4$] (e), dried MAO (f).

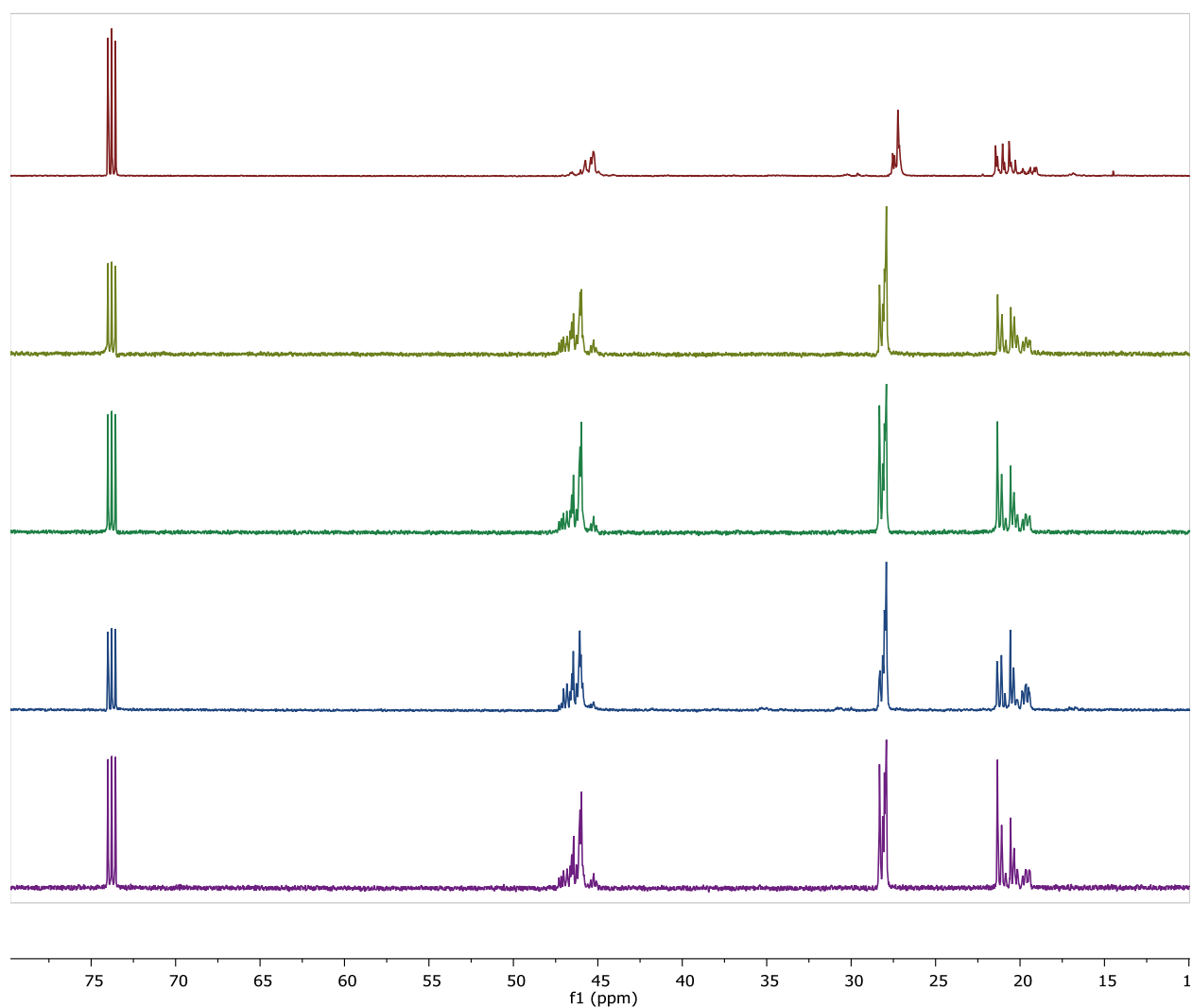


Figure S25. $^{13}\text{C}\{^1\text{H}\}$ NMR spectra in CD_2Cl_2 at 130°C of high temperature propylene homopolymers from: (top to bottom) $\text{Zr}_1^{\text{ArSiPr}_3}\text{-NMe}_2$, $\text{C}_S\text{Zr}_2^{\text{SiPr}_3}\text{-NMe}_2$, $\text{C}_2\text{Zr}_2^{\text{SiPr}_3}\text{-NMe}_2$, $\text{anthZr}_1^{\text{SiPr}_3}\text{-NMe}_2$, $\text{anthZr}_2^{\text{SiPr}_3}\text{-NMe}_2$.

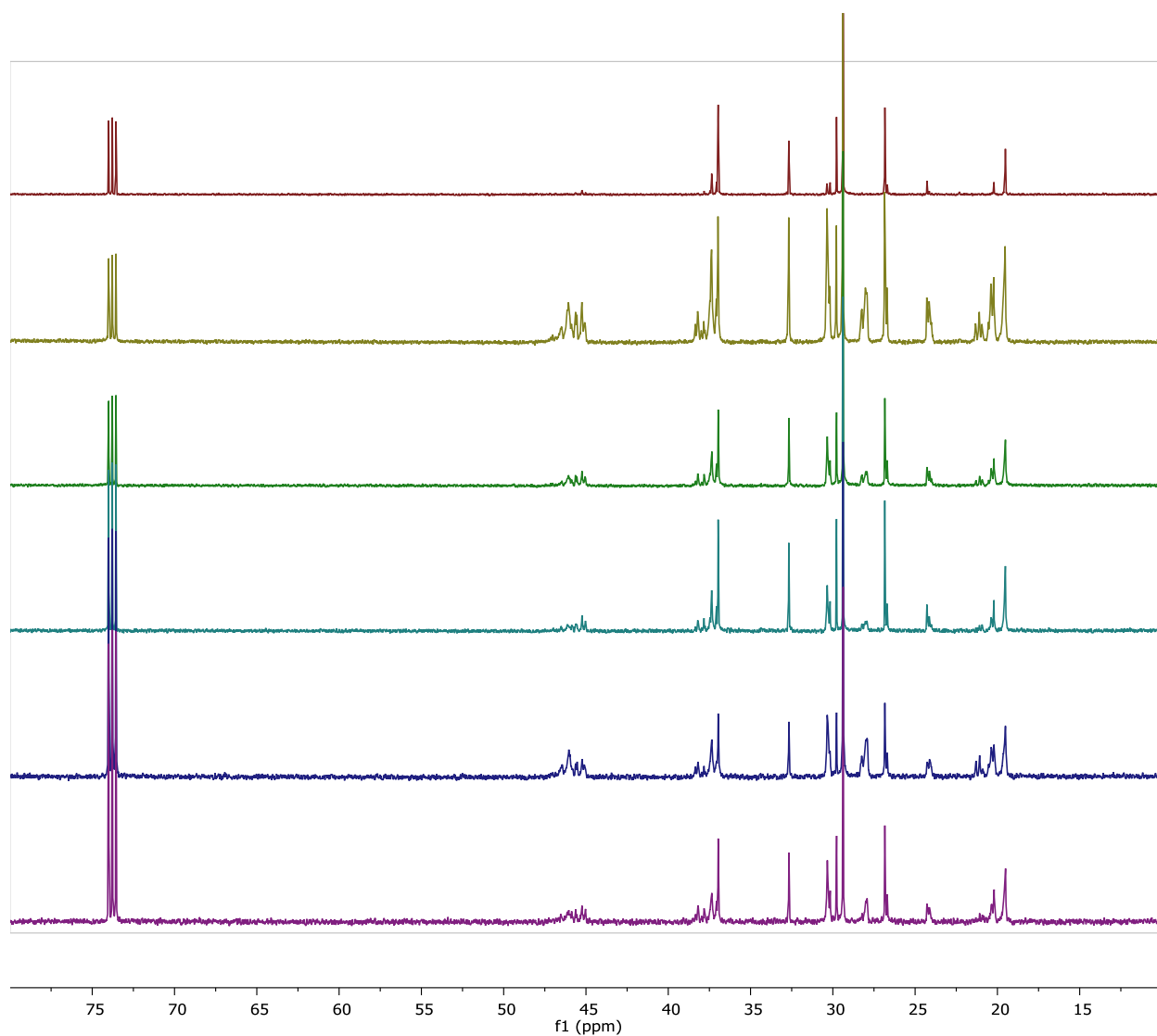


Figure S26. $^{13}\text{C}\{^1\text{H}\}$ NMR spectra in CD_2Cl_2 at 130°C of ethylene-propylene copolymers from: (top to bottom) $\text{Zr}_1^{\text{ArSiPr}_3}\text{-NMe}_2$, $\text{C}_S \text{Zr}_2^{\text{SiPr}_3}\text{-NMe}_2$, $\text{C}_2 \text{Zr}_2^{\text{SiPr}_3}\text{-NMe}_2$, $\text{anthZr}_1^{\text{SiPr}_3}\text{-NMe}_2$, $\text{anthZr}_2^{\text{SiPr}_3}\text{-NMe}_2$.

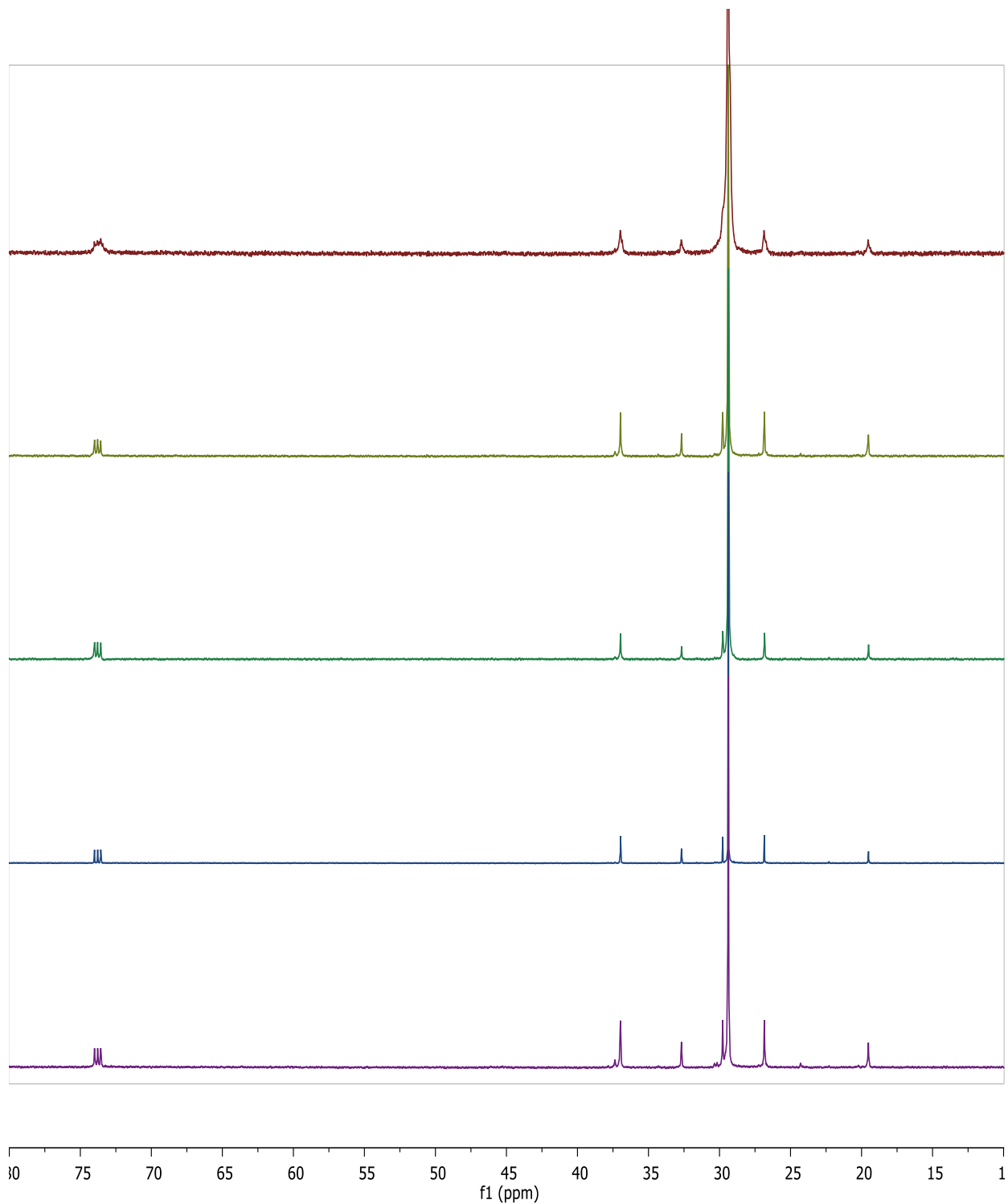


Figure S27. $^{13}\text{C}\{^1\text{H}\}$ NMR spectra in CD_2Cl_2 at 130°C of ethylene-propylene copolymers from: (top to bottom) $\text{pyZr}_1^{\text{ArSiPr}_3}$ (2), $\text{pyZr}_2^{\text{SiPr}_3}$, $\text{pyZr}_1^{\text{ArSiPh}_3}$, $\text{pyZr}_2^{\text{SiPh}_3}$.

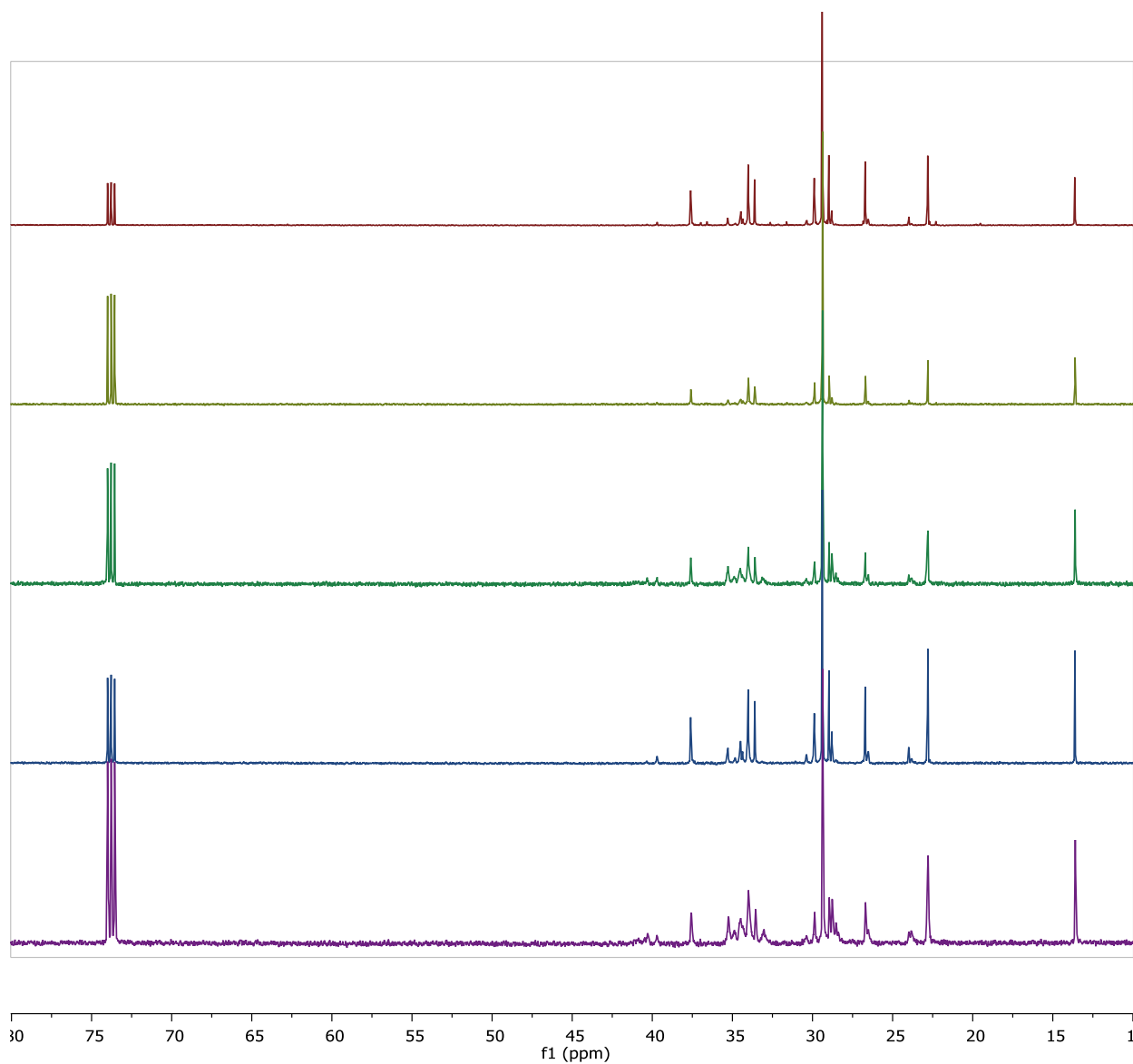


Figure S28. $^{13}\text{C}\{^1\text{H}\}$ NMR spectra in CD_2Cl_2 at 130°C of ethylene-hexene copolymers from: (top to bottom) $\text{Zr}_1^{\text{ArSiPr}_3}\text{-NMe}_2$, $\text{C}_S\text{Zr}_2^{\text{SiPr}_3}\text{-NMe}_2$, $\text{C}_2\text{Zr}_2^{\text{SiPr}_3}\text{-NMe}_2$, $\text{anthZr}_1^{\text{SiPr}_3}\text{-NMe}_2$, $\text{anthZr}_2^{\text{SiPr}_3}\text{-NMe}_2$.

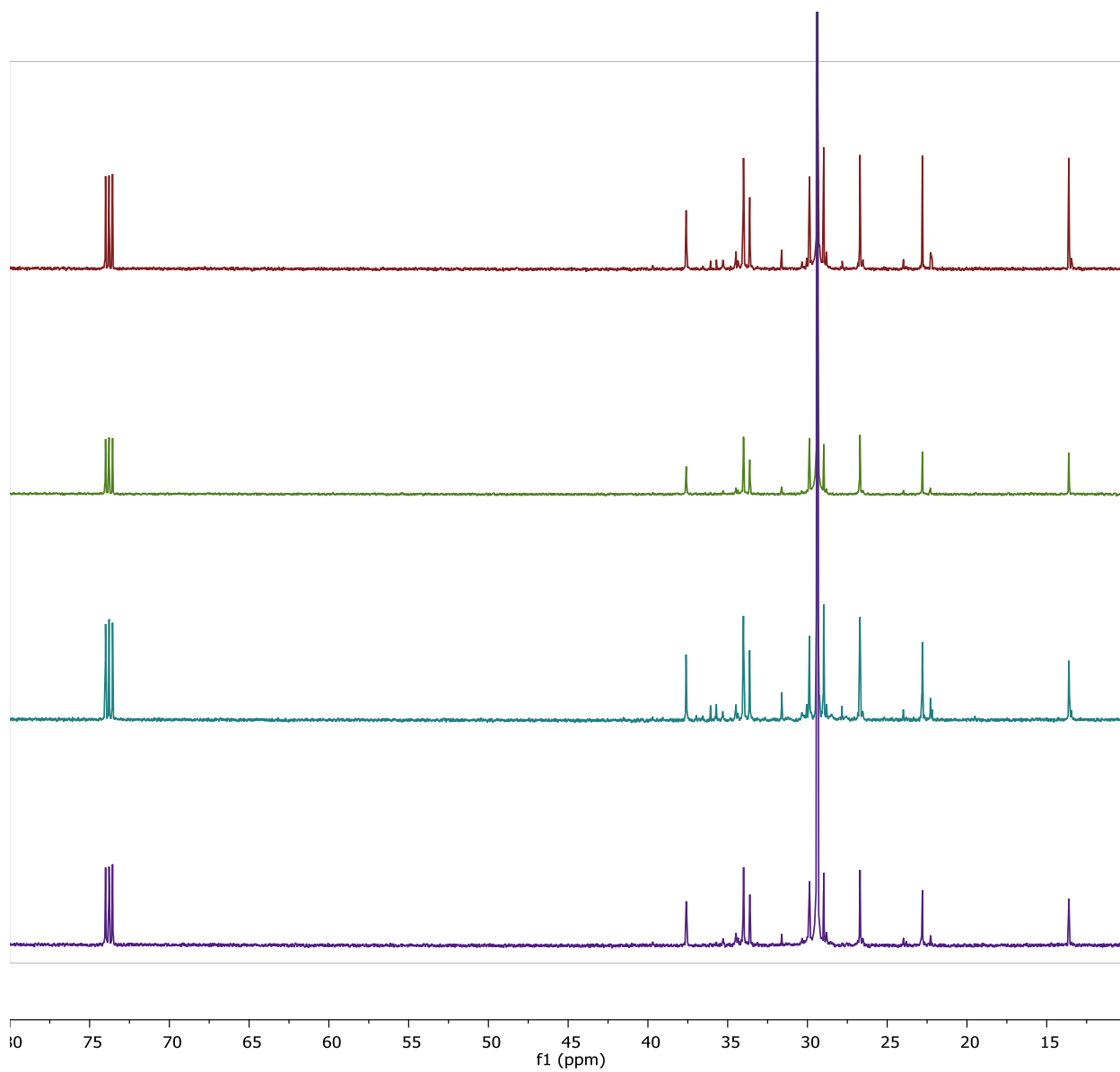


Figure S29. $^{13}\text{C}\{^1\text{H}\}$ NMR spectra in CD_2Cl_2 at 130°C of ethylene-hexene copolymers from: (top to bottom) $\text{pyZr}_1^{\text{ArSiPr}_3}$, $\text{pyZr}_2^{\text{SiPr}_3}$, $\text{pyZr}_1^{\text{ArSiPh}_3}$, $\text{pyZr}_2^{\text{SiPh}_3}$.

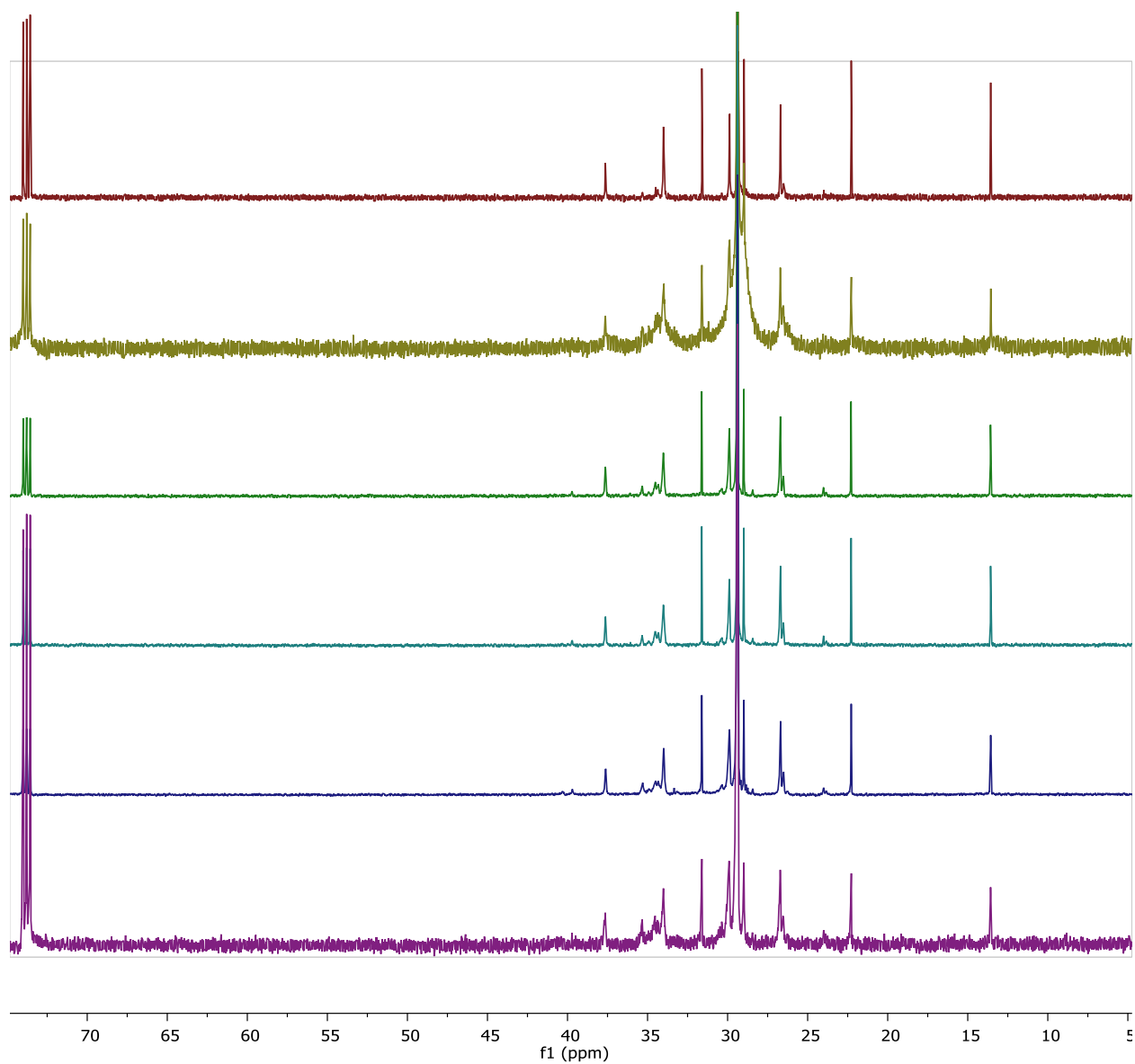


Figure S30. $^{13}\text{C}\{^1\text{H}\}$ NMR spectra in CD_2Cl_2 at 130°C of ethylene-tetradecene copolymers from: (top to bottom) $\text{Zr}_1^{\text{ArSiPr}_3}\text{-NMe}_2$, $\text{C}_S \text{Zr}_2^{\text{SiPr}_3}\text{-NMe}_2$, $\text{C}_2 \text{Zr}_2^{\text{SiPr}_3}\text{-NMe}_2$, $\text{anthZr}_1^{\text{SiPr}_3}\text{-NMe}_2$, $\text{anthZr}_2^{\text{SiPr}_3}\text{-NMe}_2$.

Polymer Tables

Table S1. Ethylene-propylene copolymerization by $\text{Zr}_1^{\text{t}^{\text{BiSi}^{\text{i}}\text{Pr}^3}}\text{-NMe}_2$.

Entry	C2:C3	Temp (°C)	Coactivator	Time (min)	Yield (g)	Activity (kg mmol_{Zr}⁻¹ h⁻¹)	% Incorporation
1	50:50	30	AlMe ₃	60	3	0.3	32
2	50:50	30	None	60	8	0.8	34
3	50:50	60	None	60	16	1.6	22
4	50:50	80	None	60	14	1.4	43
5	25:75	30	None	38	5	0.8	46
6	25:75	60	None	60	11	1.1	45
7	25:75	80	None	60	13	1.3	35

Conditions: 10 μmol Zr, 1000 equiv. MAO, 5 bar total pressure, 60 mL toluene.

Table S2. 1-Hexene and Propylene Homopolymerization

Entry	Catalyst	Monomer	Activator	Yield (g)	Activity (kg mmol _{Zr} ⁻¹ h ⁻¹)	% <i>mmmm</i> ^c	M _n	PDI
1	Zr ₁ ^{ArSiPr₃} -NMe ₂	1-Hexene	[CPh ₃] [B(C ₆ F ₅) ₄]	0.076	0.11	34	11, 39 ^d	1.2, 1.2 ^d
2	Zr ₁ ^{ArSiPr₃} -NMe ₂	1-Hexene	[HNMe ₂ Ph] [B(C ₆ F ₅) ₄]	0.046	0.069	37	10	1.3
3	Zr ₁ ^{ArSiPr₃} -NMe ₂	1-Hexene	MAO	0.116	0.17	40	11	1.3
4	C ₈ Zr ₂ ^{SiPr₃} -NMe ₂	1-Hexene	[CPh ₃] [B(C ₆ F ₅) ₄]	0.067	0.10	45	119	3.8
5	C ₈ Zr ₂ ^{SiPr₃} -NMe ₂	1-Hexene	[HNMe ₂ Ph] [B(C ₆ F ₅) ₄]	0.238	0.36	45	398	3.2
6	C ₈ Zr ₂ ^{SiPr₃} -NMe ₂	1-Hexene	MAO	0.613	0.92	10	24	3.9
7	C ₂ Zr ₂ ^{SiPr₃} -NMe ₂	1-Hexene	[CPh ₃] [B(C ₆ F ₅) ₄]	0.513	0.77	34	204	1.9
8	C ₂ Zr ₂ ^{SiPr₃} -NMe ₂	1-Hexene	[HNMe ₂ Ph] [B(C ₆ F ₅) ₄]	0.596	0.89	34	386	2.1
9	C ₂ Zr ₂ ^{SiPr₃} -NMe ₂	1-Hexene	MAO	0.676	1.0	15	28	3.8
10	anthZr ₁ ^{ArSiPr₃} -NMe ₂	1-Hexene	[CPh ₃] [B(C ₆ F ₅) ₄]	0.036	0.054	5	55, 15, 18	4.5, 1.4, 1.5
11	anthZr ₁ ^{ArSiPr₃} -NMe ₂	1-Hexene	[HNMe ₂ Ph] [B(C ₆ F ₅) ₄]	0.046	0.069	3	22, 16 ^d	14, 1.4 ^d
12	anthZr ₁ ^{ArSiPr₃} -NMe ₂	1-Hexene	MAO	0.204	0.31	4	30, 14 ^d	11, 1.4 ^d
13	C ₂ anthZr ₂ ^{SiPr₃} -NMe ₂	1-Hexene	[CPh ₃] [B(C ₆ F ₅) ₄]	0.870	1.3	28	229	2.0
14	C ₂ anthZr ₂ ^{SiPr₃} -NMe ₂	1-Hexene	[HNMe ₂ Ph] [B(C ₆ F ₅) ₄]	0.980	1.5	33	258	2.4
15	C ₂ anthZr ₂ ^{SiPr₃} -NMe ₂	1-Hexene	MAO	0.860	1.3	42	83	3.0
16	Zr ₁ ^{ArSiPr₃} -NMe ₂	Propylene	MAO	5.5	0.55	13.8	1.1	10.7
17	C ₈ Zr ₂ ^{SiPr₃} -NMe ₂	Propylene	MAO	19	1.9	18.8	10	19.1
18	C ₂ Zr ₂ ^{SiPr₃} -NMe ₂	Propylene	MAO	21.6	2.2	25.4	12	12.9
19	anthZr ₁ ^{ArSiPr₃} -NMe ₂	Propylene	MAO	9.6	0.96	14.6	7.6	4.0
20	C ₂ anthZr ₂ ^{SiPr₃} -NMe ₂	Propylene	MAO	28	2.8	23.8	26	4.5

. 1-Hexene polymerizations were run with 4.0 μmol Zr, 1 equiv. [B(C₆F₅)₄] activator or 250 equiv. dried MAO, and 5000 equiv. (2.5 mL) 1-hexene in 2.5 mL PhCl for 10 min and propylene polymerizations were run with 10 μmol Zr, 1000 equiv. (2.5 mL) MAO and 5 bar propylene in 85 mL toluene for 60 min; ^bFrom GPC analysis where PDI = M_w/M_n; ^cFrom integration of the ¹³C{¹H} NMR spectra. ^dMultimodal distribution observed.

Table S3. 1-Hexene and 1-Tetradecene Copolymerization.

Entry	Catalyst	Comonomer	Yield (g)	Activity kg (mmol Zr) ⁻¹ h ⁻¹	M _n ^b (kDa)	PDI ^b	T _m (°C)	% I ^c
1	Zr ₁ ^{ArSiPr³} -NMe ₂	1-Hexene	15.3	1.5	2.2	3.6	104	19
2	C ₈ Zr ₂ ^{SiPr³} -NMe ₂	1-Hexene	19	1.9	5.9	3.7	99	12
3	C ₂ Zr ₂ ^{SiPr³} -NMe ₂	1-Hexene	19.5	2.0	8.8	11.9	105	22
4	anthZr ₁ ^{SiPr³} -NMe ₂	1-Hexene	23.8	2.4	7.1	3.4	--	28
5	C ₂ anthZr ₂ ^{SiPr³} -NMe ₂	1-Hexene	19.2	1.9	11	8.8	104	30
6	pyZr ₁ ^{ArSiPr³}	1-Hexene	19.7	2.0	1.6	7.2	115	7
7	pyZr ₂ ^{SiPr³}	1-Hexene	14.2	1.4	3.5	18	125	4
8	pyZr ₁ ^{ArSiPh³}	1-Hexene	28.6	2.9	0.8	11	112	7
9	pyZr ₂ ^{SiPh³}	1-Hexene	19.2	1.9	1.9	35	121	5
10	Zr ₁ ^{ArSiPr³} -NMe ₂	1-Tetradecene	9.7	0.97	17	8.8	61	7
11	C ₈ Zr ₂ ^{SiPr³} -NMe ₂	1-Tetradecene	20.4	2.0	41			6
12	C ₂ Zr ₂ ^{SiPr³} -NMe ₂	1-Tetradecene	20.3	2.0	39	26	104	3
13	anthZr ₁ ^{SiPr³} -NMe ₂	1-Tetradecene	24.5	2.5	12	2.7	110	10
14	anthZr ₁ ^{SiPr³} -NMe ₂	1-Tetradecene	23.7	2.4	15	2.9	117	9
15	C ₂ anthZr ₂ ^{SiPr³} -NMe ₂	1-Tetradecene	22.5	2.3	22	6.6	105	7
16	C ₂ anthZr ₂ ^{SiPr³} -NMe ₂	1-Tetradecene	22.9	2.3	34	5.8	106	8

Polymerizations were run with 10 μmol Zr in 65 mL toluene in the presence of 1000 equiv. (2.5 mL) MAO and 3 bar ethylene and 20 mL (1.6 x 10⁵ equiv.) 1-hexene or 20 mL (7900 equiv.) 1-tetradecene at 60 °C; ^bM_n and PDI determined from GPC measurements, where PDI is defined as M_w/M_n; ^c calculated from DSC measurements; ^d% incorporation of the comonomer as identified.

Crystallographic Information

CCDC deposition numbers 1529994, 1529995, and 1529996 contain the supplementary crystallographic data for this paper. These data can be obtained free of charge from the Cambridge Crystallographic Data Centre via www.ccdc.cam.ac.uk/data_request/cif.

Refinement Details: Crystals were mounted on a glass fiber or MiTeGen loop using Paratone oil, then placed on the diffractometer under a nitrogen stream. Diffractometer manipulations, including data collection, integration, and scaling were performed using the Bruker APEXII software⁸. Absorption corrections were applied using SADABS or TWINABS (**anthZr₂^{SiiPr3}-NMe₂**)⁹. Space groups were determined on the basis of systematic absences and intensity statistics and the structures were solved in the Olex 2 software interface¹⁰ by intrinsic phasing using XT (incorporated into SHELXTL)¹¹ and refined by full-matrix least squares on F². All non-hydrogen atoms were refined using anisotropic displacement parameters. Hydrogen atoms were placed in the idealized positions and refined using a riding model. Graphical representation of structures with 50% probability thermal ellipsoids were generated using Diamond 3 visualization software¹². **Zr₁^{ArSiiPr3}-NMe₂** had disorder associated with one *tert*-butyl group and the ethylene diamine group and both sets of disorder were both modeled in two parts. **Zr₂^{SiiPr3}-NMe₂** was treated as a racemic twin and electron density corresponding to co-crystallized solvent was observed in the lattice. As these could not be satisfactorily modeled, the SQUEEZE protocol contained with the program PLATON¹³ was used to generate a bulk solvent correction to the observed intensities. Both *tert*-butyl groups, the ethylene dimethylamine group, and one benzyl group were modeled in two parts and restraints were used to bring the displacement parameters of these groups to acceptable sizes. **anthZr₂^{SiiPr3}-NMe₂** was integrated as a 50-50 twin and the co-crystallized toluene molecules were modeled in two parts and constrained to bring the displacement parameters to acceptable sizes. The disordered benzyl group was modeled in two parts and restraints were used to bring displacement parameters to acceptable sizes.

Table S4. Crystal and refinement data for $\text{Zr}_1^{\text{ArSiPr}_3}\text{-NMe}_2$, $\text{Zr}_2^{\text{SiPr}_3}\text{-NMe}_2$, and $\text{anthZr}_2^{\text{SiPr}_3}\text{-NMe}_2$.

	$\text{Zr}_1^{\text{ArSiPr}_3}\text{-NMe}_2$	$\text{Zr}_2^{\text{SiPr}_3}\text{-NMe}_2$	$\text{anthZr}_2^{\text{SiPr}_3}\text{-NMe}_2$
CCDC Number	1529995	1529994	1529996
Empirical formula	$\text{C}_{69}\text{H}_{95}\text{N}_2\text{O}_2\text{SiZr}$	$\text{C}_{108}\text{H}_{154}\text{N}_4\text{O}_4\text{Si}_2\text{Zr}_2$	$\text{C}_{126}\text{H}_{166}\text{N}_4\text{O}_4\text{Si}_2\text{Zr}_2$
Formula weight	1103.77	1810.96	2039.26
T (K)	100.01	99.98	100
a, Å	9.0866(14)	15.1120(6)	15.3649(10)
b, Å	11.0615(17)	22.3907(10)	18.5121(12)
c, Å	32.200(5)	34.1289(16)	22.6331(15)
α , °	86.076(3)	90	75.488(4)
β , °	89.449(4)	90	73.031(4)
γ , °	77.974(3)	90	73.114(4)
Volume, Å ³	3158.0(8)	11548.1(9)	5794.4(7)
Z	2	4	2
Crystal system	triclinic	orthorhombic	triclinic
Space group	P-1	I222	P-1
d_{calc} , g/cm ³	1.161	1.042	1.160
θ range, °	3.774 to 73.662	2.360 to 79.497	2.85 to 50.802
μ , mm ⁻¹	0.237	2.018	0.252
Abs. Correction	Semi-empirical	Semi-empirical	Semi-empirical
GOF	1.042	1.053	1.033
R_1 , ^a wR_2 ^b [$I > 2 \sigma(I)$]	0.0446, 0.1021	0.0455, 0.1055	0.0470, 0.0992
Radiation Type	Mo K α	Cu K α	Mo K α

$$^a R_1 = \frac{\sum ||F_o| - |F_c||}{\sum |F_o|}, \quad ^b wR_2 = \frac{[\sum [w(F_o^2 - F_c^2)^2]]^{1/2}}{[\sum [w(F_o^2)^2]]^{1/2}}.$$

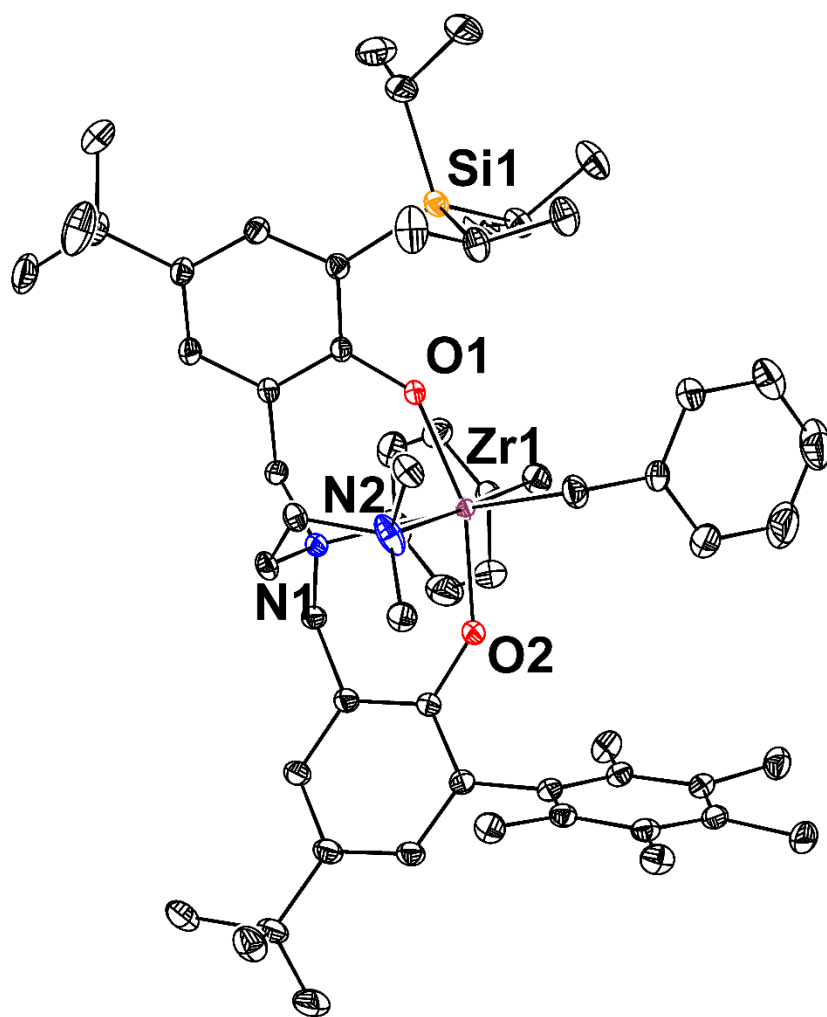


Figure S31. Structural drawing of $\text{Zr}_1^{\text{ArSiPr}_3}\text{-NMe}_2$ with 50% probability anisotropic displacement ellipsoids. Co-crystallized benzene molecules and hydrogen atoms are omitted for clarity. The minor populations of the disordered *tert*-butyl and ethylenediamine are omitted for clarity.

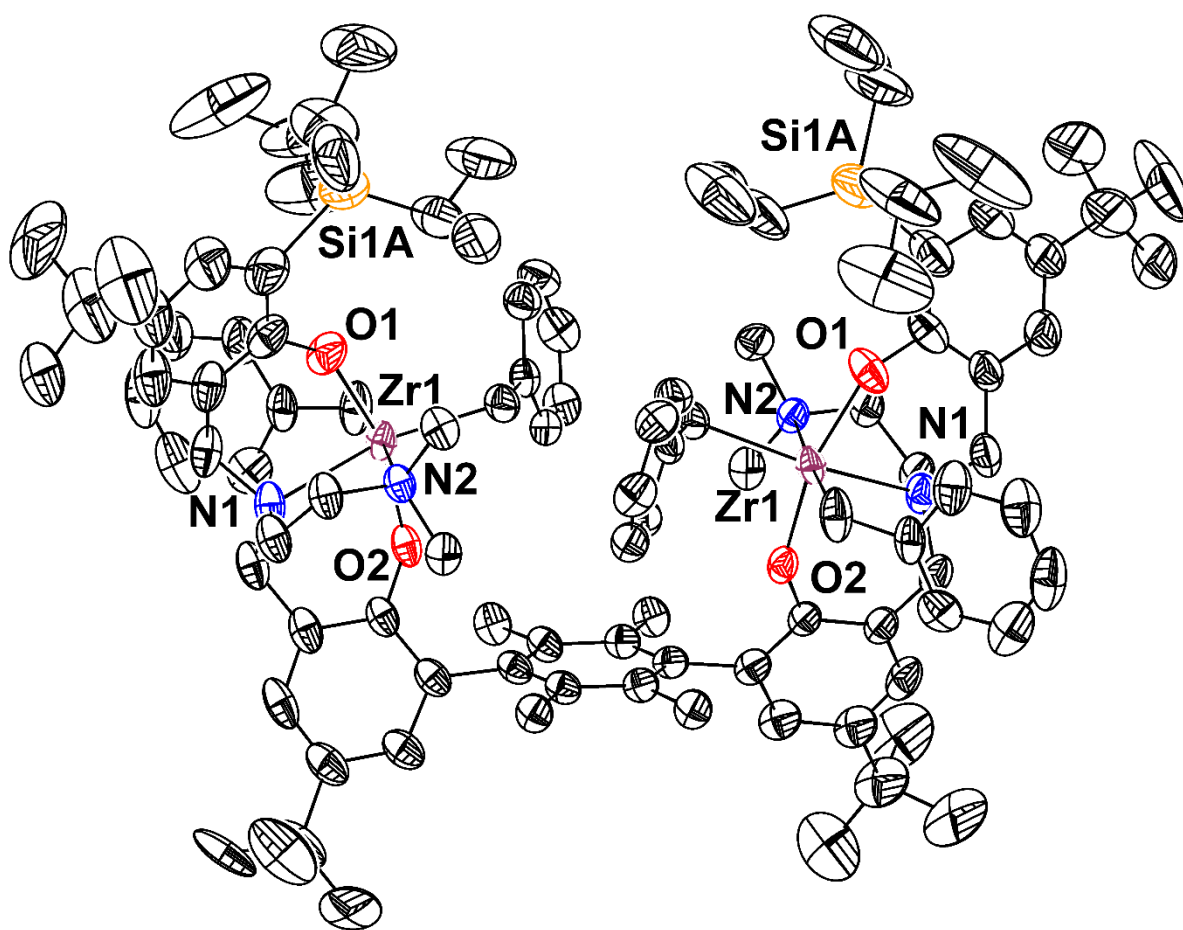


Figure S32. Structural drawing of $Zr_2^{SiPr_3-NMe_2}$ with 50% probability anisotropic displacement ellipsoids. Only the major populations of the disordered *tert*-butyl groups, the disordered benzyl, and the disordered ethylene dimethylamine are shown for clarity. Hydrogen atoms are omitted for clarity.

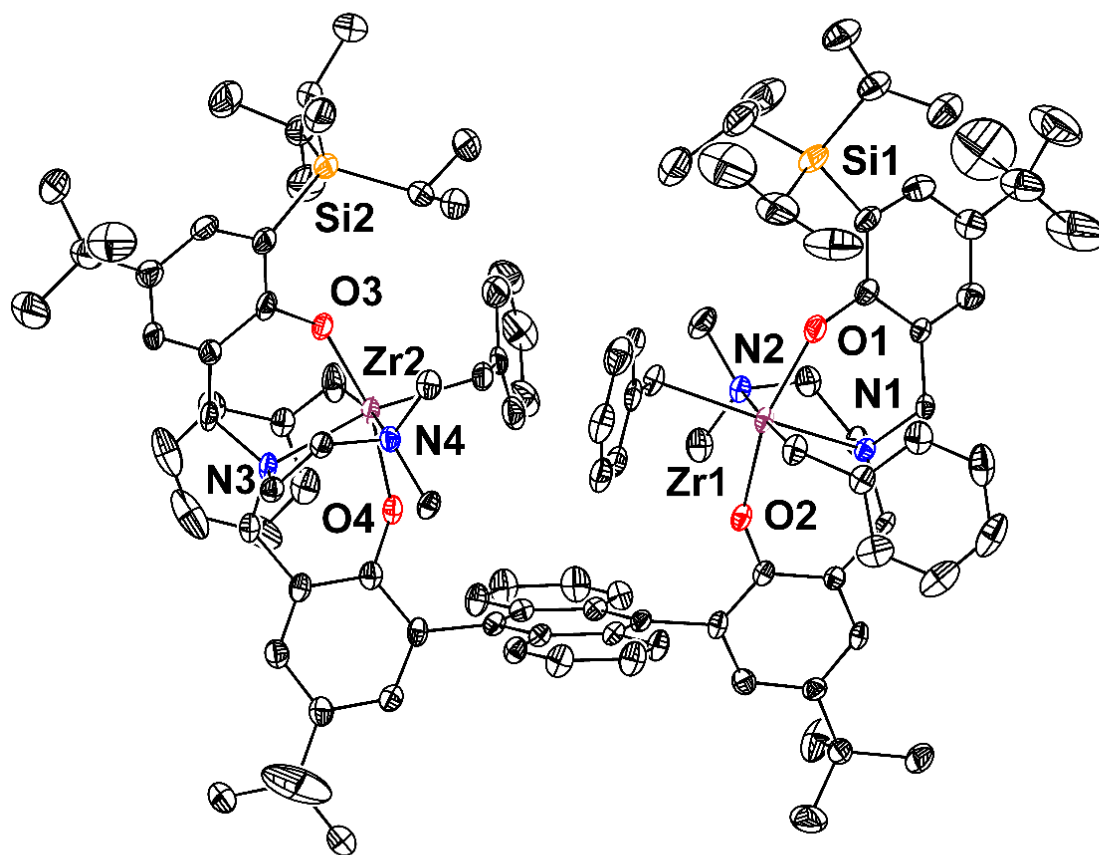


Figure S33. Structural drawing of $\text{anthZr}_2^{\text{SiPr}_3}\text{-NMe}_2$ with 50% probability anisotropic displacement ellipsoids. Only the major component of the disordered benzyl group is shown for clarity. The co-crystallized toluene molecules and hydrogen atoms are omitted for clarity.

References

1. Zysman-Colman, E.; Arias, K.; Siegel, J.S. *Can. J. Chem.* **2009**, *87*, 440-447.
2. Christensen, P.R.; Patrick, B.O.; Caron, E.; Wolf, M.O. *Angew. Chem. Int. Ed. Engl.* **2013**, *52*, 12946-12950.
3. Radlauer, M.R.; Day, M.W.; Agapie, T. *Organometallics* **2012**, *31*, 2231-2243.
4. Appiah, W.O.; DeGreeff, A.D.; Razidlo, G.L.; Spessard, S.J.; Pink, M.; Young, V.G.; Hofmeister, G.E. *Inorg. Chem.*, **2002**, *41*, 3656-3667.
5. Baldwin, D.; Gates, P.S., Process for preparing pyrogallol. Google Patents: 1979.
6. Radlauer, M.R.; Agapie, T. *Organometallics* **2014**, *33*, 3247-3250.
7. Thadani, A.N.; Huang, Y.; Rawal, V.H. *Org. Lett.* **2007**, *9*, 3873-3876.
8. APEX2, Version 2 User Manual, M86-E01078, Bruker Analytical X-ray Systems, Madison, WI, June 2006.
9. Sheldrick, G.M. "SADABS (version 2008/l): Program for Absorption Correction for Data from Area Detector Frames", University of Göttingen, 2008.
10. Dolomanov, O.V.; Bourhis, L.J.; Gildea, R.J.; Howard, J.A.K.; Puschmann, H. *J. Appl. Cryst.* **2009**, *42*, 339.
11. Sheldrick, G.M. (2008). *Acta Cryst.* A64, 112-122.
12. Brandenburg, K. (1999), DIAMOND. Crystal Impact GdR, Bonn, Germany.
13. Spek, A.L. "PLATON – A Multipurpose Crystallographic Tool, Utrecht University", Utrecht, the Netherlands, 2006.